Spring 2018

Data analysis of low-salinity waterflooding to enhance the oil recovery in sandstone reservoirs

Nadia Ariani

Department:

DATA ANALYSIS OF LOW-SALINITY WATERFLOODING TO ENHANCE THE OIL RECOVERY IN SANDSTONE RESERVOIRS

by

NADIA ARIANI

A THESIS

Presented to the Graduate Faculty of the

MISSOURI UNIVERSITY OF SCIENCE AND TECHNOLOGY

In Partial Fulfillment of the Requirements for the Degree

MASTER OF SCIENCE

in

PETROLEUM ENGINEERING

2018

Approved by

Mingzhen Wei, Advisor
Baojun Bai
Ralph E. Flori, Jr

ABSTRACT

The lack of a single reasonable general mechanism to describe how low-salinity waterflooding can improve oil recovery in both laboratory and field pilot projects has increased the interests of many researchers and stakeholders. There has not been observed the relationship of formation brine salinity and injected brine salinity to see how much salinity is reduced to produce the maximum enhanced oil recovery by LSWF. There is no guidance in what EOR stage the LSWF is best implemented. This work collects data from various published literature to develop a comprehensive data set regarding low-salinity waterflooding in sandstone reservoirs. The LSWF mechanisms are discussed to gain better understanding of the LSWF effect on oil recovery in sandstone reservoirs. The data set consists of parameters from coreflooding experiments that involved core samples, crude oil, and brines from different places. Histograms and box plots are used to visualize various kinds of data, and cross plots and charts are used to analyze the relationship between the important parameters and oil recovery. This study revealed the complexity of LSWF mechanisms and the corresponding parameters in the COBR system that associate with this process. The effects of rock porosity and permeability, total clay content, core aging temperature, COBR wettability, initial water saturation, oil base/acid ratio, asphaltenes content, formation and injected brine salinity and composition on the enhanced oil recovery are discussed in both secondary and tertiary LSWF modes. The applicability of parameters affecting the LSWF process are summarized. It is also observed the relationship between formation brine salinity and how much injected brine salinity was reduced or diluted to produce the maximum incremental secondary and additional tertiary recovery. Finally, in comparison to the conventional waterflooding, the final recovery from all of the LSWF stages are higher than the one of the conventional waterflooding, and the secondary+tertiary EOR stage produces the highest final recovery.

ACKNOWLEDGMENTS

First, I thank God for His Grace and Mercy with all my work.

I would like to thank my research advisor, Dr. Mingzhen Wei, for supporting and motivating me throughout my thesis. Her patience and understanding helped me passing through the process.

I also thank Dr. Baojun Bai for all his valuable advice and support during my master's program and thesis.

I would also like to express my thanks to Dr. Ralph Flori for his valuable advice, especially in starting the analysis part of my research.

Furthermore, I express gratitude to my colleagues in the EOR Data Group and friends in the US and Indonesia for their support.

I dedicate very special thanks to my beloved family, and my parents and brothers in Indonesia. Their love, prayers and support are endless.

TABLE OF CONTENTS

Page

LIST OF ILLUSTRATIONS

Figure Page

LIST OF TABLES

NOMENCLATURE

Symbol	Description
BP	British Petroleum
CEC	Cation exchange capacity
COBR	Crude oil/brine/rock
cP	Centipoise
E_A	Areal sweep (displacement) efficiency
E_D	Microscopic displacement efficiency
EDL	Electric double layer
E	Overall displacement efficiency
E_I	Vertical sweep (displacement) efficiency
EOR	Enhanced oil recovery
E_V	Macroscopic displacement efficiency
F_c	Capillary force
F_v	Viscous force
FW	Formation water
GUPCO	Gulf of Suez Petroleum Company
HS	High salinity
IAH	Amott-Harvey relative displacement index

IFT	Interfacial tension
I_o	Displacement-by-oil index
IOR	Improved oil recovery
I_w	Displacement-by-water index
K	Absolute permeability
K_{air}	Air permeability
K_o	Effective permeability of oil
K_{ri}	Relative permeability of phase i
K_{ro}	Relative permeability of the porous medium to oil
K_{row}	Water and oil relative permeability
K_{rw}	Relative permeability of the porous medium to water
K_w	Effective permeability of water
λ_D	Mobility of the displacing fluid phase
λ_d	Mobility of the displaced fluid phase
λ_i	Mobility of the fluid phase
$LoSal^{TM}$	BP's low-salinity water trademark
LS	Low salinity
LSWF	Low-salinity waterflooding
LSW	Low-salinity water
mD	Millidarcy

MIE	Multicomponent ionic exchange
M	Mobility ratio
μ	Viscosity
μ_i	Viscosity of phase *i*
μ_w	Viscosity of the water phase
N_{ca}	Capillary number
OOIP	Original oil-in-place
P_c	Capillary pressure
P_{cow}	Oil/water capillary pressure
$P_{non-wetting}$	Pressure in the non-wetting phase
P_o	Oil phase pressures
P_w	Water phase pressures
$P_{wetting}$	Pressure in the wetting phase
r	Radius of the capillary or pore channel
SARA	Saturates, aromatics, resins, and asphaltanes
S_{wir}	Irreducible water saturation
S_{wi}	Initial water saturation
S_o	Oil saturation
σ_{os}	Interfacial tension between oil and the solid surface
S_{or}	Residual oil saturation

S_{orw}	Residual oil to waterflood
σ_{ow}	Interfacial tension between oil and water
STOIIP	Stock tank original oil-in-place
σ	Surface tension
SWCTT	Single well chemical tracer test
σ_{ws}	Interfacial tension between water and the solid surface
SW	Sea water
TAN	Total acid number
TBN	Total base number
TDS	Total dissolved solids
θ	Measured contact angle; measure of LS vs. HS character
v	Interstitial velocity
V_{osp}	Oil volume displaced by spontaneous water imbibition
V_{ot}	Total oil displaced by water imbibition and forced displacement
V_{wsp}	Water volume displaced by spontaneous oil imbibition
V_{wt}	Total water displaced by oil imbibition and forced displacement

1. INTRODUCTION

Waterflooding is a secondary oil recovery method that is still very common in the industry. This technique is a successful and widely used enhanced oil recovery process. It is understandable that compared to other fluids, water is widely available, inexpensive, easy to inject, environmental friendly, and very efficient in displacing oil. Nevertheless, a tertiary effect of waterflooding has been observed lately, depending on the composition and salinity of the injected water. The literature shows that the adjustment of brine composition injected into a reservoir in the waterflooding process can increase oil recovery. This means that the quality of injected brine is important, so it should be controlled. If the salinity of injected water is monitored, the process is called a low-salinity waterflooding. This is one of the enhanced oil recovery methods that uses water with a low concentration of dissolved salts as a flooding medium.

The technology of low-salinity waterflooding (LSWF) has been proposed to improve oil recovery in many projects worldwide. Laboratory experiments and field pilot applications have shown that there is improved oil recovery corresponding to low-salinity waterflooding, compared to conventional waterflooding implementation. However, there is still no consensus on the underlying mechanism of LSWF for enhanced oil recovery. The wettability alteration is the generally accepted impact from most mechanisms. The LSWF mechanisms and their impacts, as well as their factors and contra statements, will be discussed in this thesis.

1.1. PROBLEM DEFINITION

The lack of a single reasonable general mechanism to describe how low-salinity waterflooding can improve oil recovery in both laboratory and field pilot projects has increased the interests of many researchers and stakeholders. There is no understanding as

to why it works better than the conventional high-salinity waterflooding. Many studies do not demonstrate the relationship of formation brine salinity and injected brine salinity to see how much salinity is reduced according to LSWF. There is no standard application for when LSWF should be done in the enhanced oil recovery (EOR) stage, whether it is better to implement it in the secondary stage or tertiary stage.

Furthermore, a comprehensive study of field applications in LSWF has not been done as a reference for the industry before applying the LSWF in the field. There should be a guideline of necessary conditions for the LSWF implementation.

1.2. RESEARCH OBJECTIVES

The objective of this study is to gain better understanding of the LSWF effect on enhanced oil recovery in sandstone reservoirs. This study also includes the low-salinity waterflooding mechanisms, the necessary conditions that need to be considered in a low-salinity water flooding project, to observe the relationship between formation brine salinity and injected brine salinity to see how much conventional waterflooding salinity is reduced to produce the maximum enhanced oil recovery in LSWF, and in what EOR stage the LSWF is best implemented. This study utilizes data analyses from many laboratory experiments and field cases found in the literature. Data quality issues and special case identifications are addressed by box plots and cross-plots. The data range of each parameter is shown by box plots and histograms. Finally, the correlation of some parameters is approached by cross plots and bar charts.

This thesis consists of the theory of the literature and describes the fundamental concepts that are required to understand the subject matter. The data analyses from many references support the objective above.

1.3. BRIEF DESCRIPTION OF SECTIONS

Section 2 discusses the literature review that includes the fundamental theories of oil recovery, which are primary, secondary, tertiary, and LSWF in EOR processes. It also explains the types, measurement, and mechanisms of wettability alteration by crude oil, and wettability effects on recovery by LSWF. Furthermore, Section 2 discusses the relative permeability and capillary pressure curves, salinity effects on relative permeability curves, and the influence of EOR on relative permeability curves. The crude oil/brine/rock interactions are also shown in Section 2. At the end of this section, the underlying proposed mechanisms of LSWF are discussed to show the pros and cons of each mechanism.

Section 3 presents the data set collection and visualization. The data were collected from 50 literatures for coreflooding since the published year of 1955 to 2017, whereas for field applications, the data were collected from 10 literatures since the published year of 2010 to 2016. No limitation with regards to the publication date of the references were published.

Section 4 discusses about the results analysis based on the corefloodings data set. It shows the effect of some important parameters on the oil recovery in low-salinity waterflooding process. The relationship between formation brine salinity and injected brine salinity to see how much conventional waterflooding salinity is reduced to produce the maximum enhanced oil recovery in LSWF is observed in this section. It also shows the effect of LSWF recovery stage on the final recovery.

Section 5 presents the conclusion statement based on this research work. It shows the important observation of the relationship between LSWF parameters and oil recovery in both secondary and tertiary modes. In addition, it presents some suggestions for any future work.

2. LITERATURE REVIEW

This section reviews the fundamental concepts of oil recovery, wettability, relative permeability, capillary curves, and their effects on salinity in LSWF. The purpose is not to elaborate the details in all subjects, it is to build a basic foundation that introduces most of the terms required to adequately understand the subject in this thesis. This chapter also presents the proposed underlying mechanisms of LSWF from many studies, which show the pros and cons of each mechanism.

2.1. OIL RECOVERY PROCESSES

The oil recovery process is categorized into three stages: primary, secondary, and tertiary recovery (Green and Willhite, 2008). However, since many reservoir production operations do not follow this chronological sequence, the term tertiary recovery has been replaced by a more complete term, enhanced oil recovery (EOR). Another widely used term is improved oil recovery (IOR) which includes EOR, but also encompasses other practices such as reservoir characterization, improved reservoir management, and infill drilling. Figure 2.1 shows a schematic representation of the oil recovery stages.

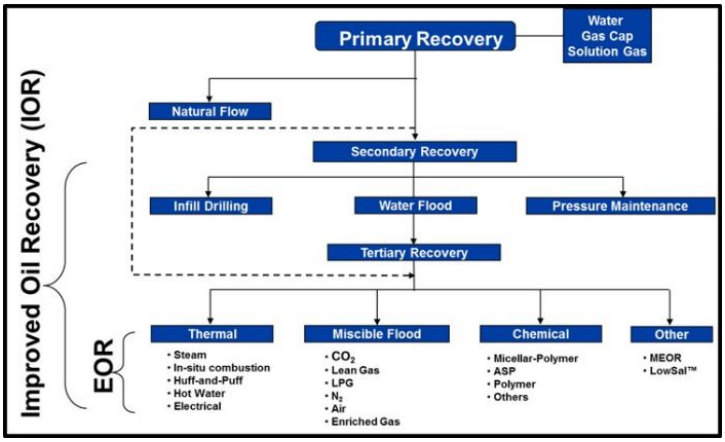

Figure 2.1. Sequential stages of oil recovery (Alvarez, 2017).

2.1.1. Primary Recovery. In the primary recovery, hydrocarbons are produced by either natural energy of the reservoir or by using pump jacks and other artificial lift devices. Green and Willhite (2008) stated that the underlying natural energy sources are as follows:

1. Solution-gas drive
2. Gas-cap drive
3. Natural water drive
4. Fluid and rock expansion
5. Gravity drainage

In fact, only around 5-15% of the original oil-in-place (OOIP) is recovered from this primary method, and it mainly depends on the type of hydrocarbons and the reservoir drive mechanism.

2.1.2. Secondary Recovery. Secondary recovery is started when natural reservoir energy is depleted to the extent that there is not enough energy to economically lift fluids (Green and Willhite, 2008). This method involves the injection of gas or water, which will displace the oil and force it to move to the surface. This is typically successful in targeting an additional 30% of the oil reserves. Secondary recovery is commonly known as waterflooding.

2.1.3. Tertiary Recovery (EOR). The way to further increase oil production is through the tertiary recovery method or EOR. The energy used in this technique is usually added to the natural or physical displacement mechanisms of the primary or secondary methods. Improved fluid flow within the reservoir is usually induced by the addition of heat, chemical interactions between the injected fluid and the reservoir fluids, mass transfer, and/or altering the oil properties in such a way that the process enhances oil movement through the reservoir. These methods are often referred to as EOR processes.

Some of the frequently used EOR processes are the following (Green and Willhite, 2008):

1. Mobility control process (provides stable mobility ratios to improve macroscopic displacement efficiency, e.g., polymer and foam injection).

2. Chemical processes (chemical injected to displace oil by interfacial tension (IFT) reduction, e.g., surfactant and alkaline injection).

3. Miscible processes (injection of fluids that are miscible with oil in the reservoir, e.g., injection of hydrocarbon solvents or CO_2).

4. Thermal processes (injection of thermal energy or in-situ generation of heat to improve oil recovery, e.g., steam injection and in-situ combustion).

5. Other processes (e.g., microbial-based techniques, immiscible CO_2 injection and mining of resources at shallow depths).

2.1.4. Low-Salinity Waterflooding (LSWF). Low-salinity waterflooding (LSWF) is an EOR technique in which the composition of the injected water is monitored in order to improve oil recovery. Low-salinity waterflooding has been proposed in many projects worldwide. Experiments in laboratory and field pilot applications have demonstrated that there is improved oil recovery associated with LSWF compared to conventional waterflooding practices.

LSWF may be applied either as a secondary or as a tertiary recovery method (McGuire *et al.* (2005); Lager *et al.* (2008a); Seccombe *et al.* (2010)). Low-salinity water such as fresh water from rivers can be injected during initial stages of production with the aim of maintaining reservoir pressure and displacing oil into production. In this case, the low-salinity injection aims to sweep out the reservoir macroscopically. LSWF may also be

implemented as an EOR technique to reduce residual oil saturation in the reservoir rock. In such a case, the purpose of applying LSWF is to increase microscopic sweep efficiency. Nevertheless, these two processes are mostly connected.

2.2. WETTABILITY

Wettability is the tendency of one fluid to preferentially adhere to a solid surface in the presence of a second fluid (Green and Willhite, 2008). When two immiscible fluid phases are placed in contact with a solid surface, one phase is usually attracted to the solid more than the other phase. The stronger attracted phase is called the wetting phase, and the less strongly attracted phase is called the non-wetting phase. Rock wettability has an impact on the nature of fluid saturations and the general relative permeability characteristics of a fluid/rock system (Green and Willhite, 2008). Changes in the wettability of a rock will affect the electrical properties, capillary pressure, relative permeability, dispersion, and simulated EOR (Anderson, 1986).

2.2.1. Measurement and Types of Wettability. There are so many quantitative and qualitative methods that have been developed to measure the wettability of a fluid/rock system. Anderson (1986) conducted a study of the quantitative methods, such as contact angle, imbibition and forced displacement (Amott), US Bureau of Mines, and electrical resistivity wettability method. The qualitative methods include microscope examination, flotation, glass slide method, relative permeability curves, permeability/saturation relationship, capillary pressure curves, capillarimetric method, displacement capillary pressure, reservoir logs, nuclear magnetic resonance, and dye adsorption.

The contact angle method is the best way to measure wettability especially when pure fluids and artificial cores are used since there is no tendency of the measured wettability being altered by surfactants or other compounds (Anderson, 1986). It is not possible to measure contact angle in porous media due to the difficulty in obtaining smooth surfaces. Nevertheless, contact angle measurements can be used to study mechanisms in the labo-

ratory. When a water droplet is placed on a surface in contact with oil, a contact angle is formed with values ranging from 0 to 180° (0 to 3.14 rad) (Anderson, 1986). The surface energies in the system are related by Young's equation as follows:

$$\sigma_{ow} cos\theta = \sigma_{os} - \sigma_{ws} \tag{2.1}$$

where σ_{ow} is the IFT between oil and water, σ_{os} is the IFT between oil and the solid surface, σ_{ws} is the IFT between water and the solid surface, and θ is the measured contact angle.

By convention, the contact angle θ is measured through the water. As shown in Figure 2.2, when the contact is less than 90° (1.6 rad), the surface is preferentially water-wet, and when it is greater than 90° (1.6 rad), the surface is said to be preferentially oil-wet. Anderson (1986) summarizes the approximate relationships between contact angle and wettability, as shown in Table 2.1.

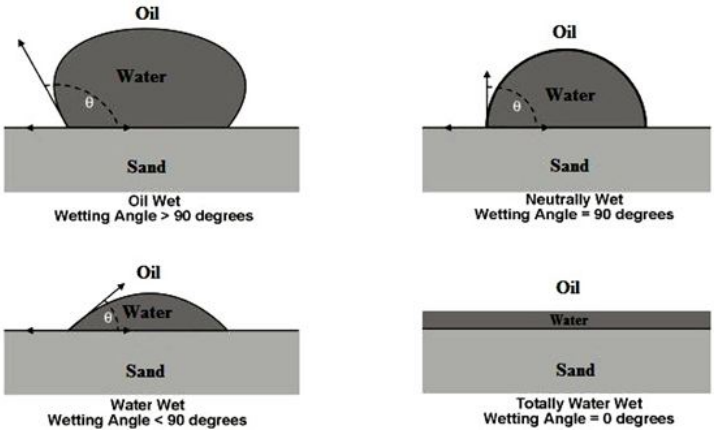

Figure 2.2. Wettability of oil/water/solid system (Kantzas *et al.*, 2016).

Table 2.1. The wettability based on contact angle (Anderson, 1986).

Contact angle	Water-wet	Neutrally wet	Oil-wet
Minimum	0	60-75°	105-120°
Maximum	60-75°	105-120°	180°

Another commonly used wettability measurement method is the Amott test. It is a test to determine the average wettability of a core, which involves imbibition and forced displacement volumes for both water by oil and oil by water. The wettability of the rock according to the Amott's test is giving by two ratios. The first one is displacement-by-oil index (I_o), which is a ratio between water volume displaced by spontaneous oil imbibition alone (V_{wsp}) and the total water displaced by oil imbibition and centrifugal (forced) displacement (V_{wt}), as follows:

$$I_o = \frac{V_{wsp}}{V_{wt}}. \tag{2.2}$$

The second one is displacement-by-water index (I_w), which is a ratio between oil volume displaced by spontaneous water imbibition alone (V_{osp}) and the total oil displaced by water imbibition and centrifugal (forced) displacement (V_{ot}), as follows:

$$I_w = \frac{V_{osp}}{V_{ot}}. \tag{2.3}$$

The wettability of a rock is given by these indexes. For a strong water-wet core, I_w will be positive, whereas I_o will be zero. In another way, for a strong oil-wet core, I_o will have a positive value, while I_w will be zero. In the case of a neutral wet core, both indexes are zero.

A modification of this method called the Amott-Harvey Relative Displacement Index (IAH), is used more frequently and defined as

$$IAH = I_w - I_o. \tag{2.4}$$

This index has different wettability criteria than the previous one. The range is $0.3 \leq IAH \leq 1.0$ for a water-wet system, $-0.3 \leq IAH \leq 0.3$ for an intermediate-wet system, and $-1 \leq IAH \leq -0.3$ for an oil-wet system.

However, Morrow (1990) found that reservoir wettability is not a simple defined property and thus the classification of reservoirs as either water-wet or oil-wet is oversimplification. This is because the reservoir rock surfaces are made up of a different combination of minerals with each section of the rock surface presenting different wettability to the fluids in contact with the rock.

2.2.2. Mechanism of Wettability Alteration. Buckley *et al.* (1997) stated that there are four associations in a crude oil/brine/rock system, which are as follows:

1. Polar interactions: polar components such as asphaltenes adsorb directly onto the rock surface in the absence of water film.

2. Surface precipitation: mainly dependent on crude oil solvent properties with respect to the asphaltenes and other heavy components.

3. Acid/base interactions: will occur where charges at oil/brine and rock/brine interfaces changes the pH of the system.

4. Ion binding: divalent ions such as Ca^{2+} and Mg^{2+} tend to bind oil components to brine and rock

Any conditions that are favorable for these interactions can cause the rock to be more oil wet and the water film to become very unstable as the oil components gain access to the rock surface. Nasralla and Nasr-El-Din (2012) studied that in the case of LSWF, the repulsion between the similarly charged oil/brine interface and rock surface will overcome the binding force, and causes oil desorption and a change to a more water-wet surface.

2.3. MICROSCOPIC DISPLACEMENT FORCES

One of the important aspects of the EOR process is the effectiveness of process fluids in removing oil from the rock pores at the microscopic scale. Green and Willhite (2008) describe three microscopic displacement forces for determining the fluid flow in porous media, which are as follows:

1. Capillary forces
2. Viscous forces
3. Phase trapping

An appreciation of the magnitude of these forces is required to understand the recovery mechanisms in EOR processes. The forces determine whether the fluids flow through the porous media or get trapped.

2.3.1. Capillary Forces. Green and Willhite (2008) stated that when two immiscible phases coexist in a porous medium, the surface energy related to the fluid interfaces influences the saturations, distributions, and displacement of the phases. The surface force, is quantified in terms of surface tension (σ), which is the tensile force acting in the plane of the surface per unit length of the surface. The surface tension is used for the surface between a liquid and its vapor or air. If the surface is between two different liquids, or between a liquid and a solid, it is called interfacial tension (IFT).

Despite the interfaces that are in tension in the systems, a pressure difference exists across the interface. The pressure is called capillary pressure (P_c), which is pressure in the non-wetting phase minus the pressure in the wetting phase. It can be expressed mathematically as follows:

$$P_c = P_{non-wetting} - P_{wetting}. \tag{2.5}$$

The P_c can either have positive or negative values. For a two-phase oil-water system and water is the wetting phase, the capillary pressure is defined as

$$P_c = P_o - P_w \tag{2.6}$$

where P_o and P_w are the oil and water phase pressures, respectively. The capillary pressure in an oil-water system, where oil is the non-wetting phase is further defined by Green and Willhite (2008) as

$$P_c = P_o - P_w = \frac{2\sigma_{ow} cos\theta}{r} \tag{2.7}$$

where σ_{ow} is the interfacial tension (IFT) across the oil and water interface, θ is the contact angle, and r is the radius of the capillary or pore channel. Strong capillary forces during waterflooding processes may trap oil and cause relatively high residual oil saturation. From the 2.7, the trapping oil can be reduced by lowering of the IFT by injecting surfactant or reducing $cos\theta$ by inducing a wettability alteration. LSWF may cause a wettability alteration. McGuire *et al.* (2005) stated that LSWF leads to in-situ surfactant generation, which causes IFT reduction and therefore, will reduce capillary pressure and improve fluid flow.

2.3.2. Viscous Forces. According to Green and Willhite (2008), viscous forces in a porous medium increases the magnitude of the pressure drop that occurs when a fluid flows through the medium. A fluid flows in the porous medium when the viscous force dominates the capillary and gravity forces. The viscous force is related to the capillary force through the dimensionless group called the capillary number. The capillary number for water displacing oil is defined as

$$N_{ca} = \frac{F_v}{F_c} = \frac{v\mu_w}{\sigma_{ow} cos\theta} \tag{2.8}$$

where N_{ca} is the capillary number, F_v is the viscous force, F_c is the capillary force, v is the interstitial velocity, and μ_w is the viscosity of the water phase.

Based on equation (2.8), a high capillary number is required to displace fluids. Green and Willhite (2008) observed that waterflooding operates at conditions where $N_{ca} < 10^{-6}$. At these N_{ca} values, residual oil cannot be displaced by water. However, if N_{ca} can be increased to $N_{ca} > 10^{-5}$, the residual oil can be mobilized. The capillary number is usually higher by increasing the interstitial velocity, increasing the injectant viscosity (adding polymers), by reducing the IFT (injecting surfactants), or inducing a wettability alteration to reduce the contact angle.

The IFT between water and oil can be reduced by injecting low-salinity water into formation, and LSWF can also alter the wettability of mineral surface (McGuire *et al.*, 2005). Therefore, LSWF can increase the value of N_{ca} and enhance fluid flows in the porous medium.

2.3.3. Phase Trapping. Capillary and viscous forces control phase trapping and mobilization of fluids in porous media, and therefore the microscopic displacement efficiency (Green and Willhite, 2008). The researchers explain that the trapping mechanism is known to depend on the pore structure of the porous medium, fluid/rock interactions related to wettability, and fluid/fluid interactions related to IFT.

When a wetting phase is trapped by the displaced non-wetting phase, the trapping occurs over relatively larger distances in the porous medium. In linear water floods in which oil wets the medium, this is reflected in early-water breakthrough followed by continued oil production for long periods of time. The wetting phase saturation is reduced rather slowly to a point where capillary forces dominate viscous forces and the flow ceases.

Mobilization of trapped oil and the displacement of oil can be accomplished by use of a favorable phase behavior relationship between the oil and a displacing fluid. Phase behavior relationships, for instance, can result in solubilization of a displacing fluid into the oil, resulting in the swelling of the oil volume. Relative permeability considerations can lead to improved oil recovery.

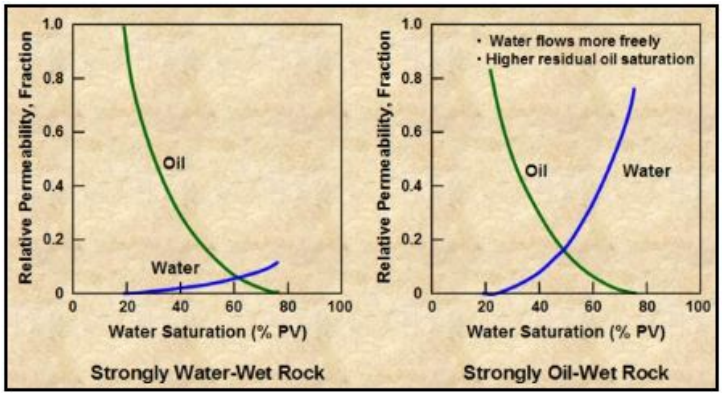

Figure 2.3. Typical relative permeability curves for water-wet and oil-wet rocks (Crain, 2015).

2.4. RELATIVE PERMEABILITY

Fluid-saturation distribution and fluid flow through porous media are strongly affected by the relative permeability and capillary pressure relationships (Green and Willhite, 2008). Relative permeability is defined as the ratio of effective permeability of the fluid at a given saturation to a base permeability (Amyx *et al.*, 1960). The base permeability may be defined as absolute permeability (K), the permeability of the porous medium saturated with a single fluid, air permeability (K_{air}), or effective permeability to non-wetting phase at irreducible wetting phase saturation. The relative permeability for oil and water can be written as follows:

$$K_{ro} = \frac{K_o}{K} \tag{2.9}$$

$$K_{rw} = \frac{K_w}{K} \tag{2.10}$$

where K_{ro} and K_{rw} are the relative permeability of the porous medium to oil and water, respectively. K_o and K_w are the effective permeability of oil and water, respectively, and K is the permeability at 100% saturation of one of the fluid phases. Figure 2.3 shows the typical relative permeability curves for water-wet and oil-wet rocks as a function of wetting phase saturation.

The relative permeability is affected by some factors, such as fluid saturations, geometry of the pore spaces and pore size distribution, and wettability and fluid saturation history (imbibition and drainage). In a strongly water-wet system, oil is expected to flow easier than in a strongly oil-wet system.

2.4.1. Salinity Effects on Relative Permeability Curves. The effect of salinity on relative permeability and capillary pressure curves is demonstrated by Jerauld *et al.* (2006). They modeled the salinity dependence of relative permeability and capillary pressure curves with simple empirical correlations. Their correlations give a good background and understanding of fluid flow in LSWF. The model assumptions are as follows:

1. Salt is modeled as an additional single-lumped component in the aqueous phase. Thus, salt can be injected and tracked, and the viscosity and density of the aqueous phase is dependent on salinity.

2. Relative permeability and capillary pressure are a function of salinity but this dependence disappears at high and low salinities. High and low-salinity relative permeability curves are made inputs and shapes are then interpolated between.

The model yields the following equations:

$$K_{rw} = \theta K_{rw}^{HS}(S^*) + (1 - \theta K_{rw}^{LS}(S^*)) \tag{2.11}$$

$$K_{row} = \theta K_{row}^{HS}(S^*) + (1 - \theta K_{row}^{LS}(S^*)) \tag{2.12}$$

$$P_{cow} = \theta P_{cow}^{HS}(S^*) + (1 - \theta P_{cow}^{LS}(S^*)) \tag{2.13}$$

$$\theta = (S_{orw} - S_{orw}^{LS})/(S_{orw}^{HS} - S_{orw}^{LS}) \tag{2.14}$$

$$S^* = (S_o - S_{orw})/(1 - S_{wir} - S_{orw}) \tag{2.15}$$

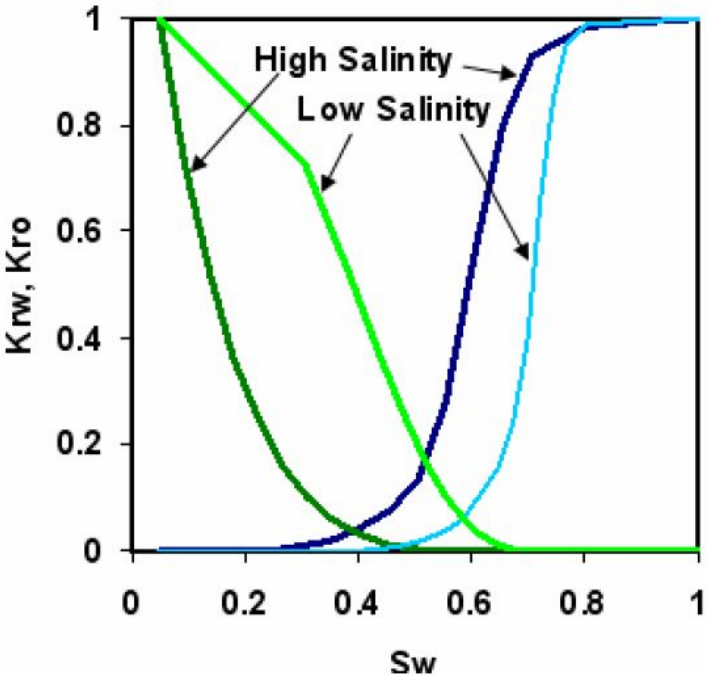

Figure 2.4. Relative permeability curves for low and high salinity system (Jerauld *et al.*, 2006).

where K_{rw} is the water relative permeability, K_{row} is the water and oil relative permeability, P_{cow} is oil/water capillary pressure, S_o is oil saturation, S_{orw} is residual oil to waterflood, S_{wir} is irreducible water saturation, and θ is a dimensionless measure of low salinity vs. high salinity character. HS and LS indicate high salinity and low salinity, respectively. The value of θ is between 0 to 1, where 0 is at low salinity and 1 is at high salinity. High- and low-salinity relative permeability and capillary pressure curves are made in between depending on the value of θ chosen. Figure 2.4 shows the typical graph of relative permeability curves with salinity dependence.

2.4.2. EOR Influences on Relative Permeability Curves. The tertiary recovery stage targets recovering the remaining oil in a reservoir after a conventional secondary recovery project, such as a water drive project, and the EOR techniques could have an effect

on the relative permeability curves (Dake, 1983), which is shown in Figure 2.5. After an ideal water drive, K_{ro} is zero when $S_o = S_{or}$ (point A in the Figure 2.5) and the oil will not flow.

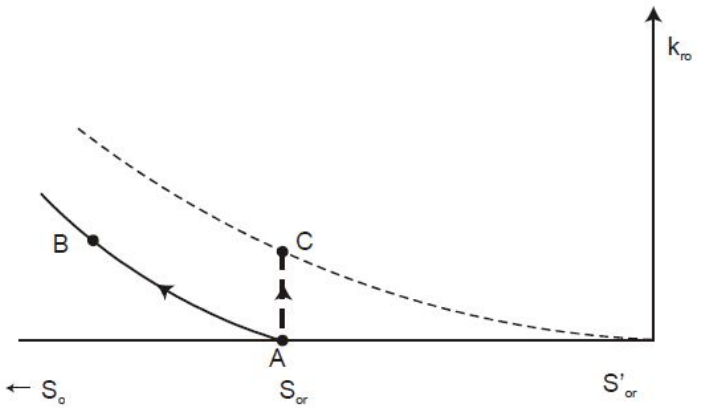

Figure 2.5. Two methods of mobilizing remaining oil after conventional waterflooding (Dake, 1983).

There are two possibilities for improving the situation and initiating the fluid flow, which are as follows:

1. The oil is displaced by fluids soluble in it. This will result in the increase of oil saturation above S_{or}. This is the same as moving from point A to B on the normal relative permeability curve, which eventually produces a finite K_{ro} and the oil becomes mobile.

2. The use of fluids which can reduce interfacial tension or have an ability to alter properties between oil and fluids. This method involves the use of miscible or semi-miscible fluids to reduce the residual oil saturation to a very low value (S'_{or}).

One of the mechanisms of LSWF proposed by McGuire *et al.* (2005) explains that during LSWF, the IFT between the injected fluid and the oil is reduced, which leads to the mobilization of residual oil.

2.5. DISPLACEMENT EFFICIENCY

Green and Willhite (2008) explained that the overall displacement efficiency of an oil recovery process can be defined as the product of microscopic and macroscopic displacement efficiencies. It is expressed mathematically as

$$E = E_D E_V \tag{2.16}$$

where E is overall displacement efficiency, and E_D and E_V are microscopic and macroscopic displacement efficiency, respectively.

Microscopic displacement refers to the mobilization of oil at the pore scale (Green and Willhite, 2008). Therefore, E_D can be defined as a measure of the effectiveness of the displacing fluid in moving the oil within spaces in the rock where the displacing fluid interacts with the oil. E_D is reflected in the magnitude of the residual oil saturation (S_{or}) in the regions contacted by the displacing fluid. Thus, E_D can be defined as

$$E_D = \frac{(1 - S_{or})}{(1 - S_{wi} - S_{or})} \tag{2.17}$$

where S_{wi} is the initial water saturation.

Green and Willhite (2008) explained that macroscopic displacement efficiency or volumetric sweep efficiency (E_V) can be considered conceptually as the product of the areal and vertical sweep efficiencies, which is expressed as

$$E_V = E_A E_I \tag{2.18}$$

where E_A is the areal sweep (displacement) efficiency in an idealized or model reservoir, or it can be said as area swept divided by total reservoir area; and E_I is the vertical sweep (displacement) efficiency, which is a pore space invaded by the injected fluid, divided by the

pore space. The macroscopic displacement efficiency describes how effective the displacing fluid is contacting the reservoir in a volumetric sense. It is also a measure of how effectively the displacing fluids moves the displaced oil towards the production wells.

The basic mechanics of oil displacement are strongly influenced by the mobility ratio, either in a miscible or immiscible displacement process. The mobility ratio (M) of any fluid is defined as

$$M = \frac{\lambda_D}{\lambda_d} \tag{2.19}$$

where λ_D is mobility of the displacing fluid phase, and λ_d is mobility of the displaced fluid phase. The mobility of the fluid phase (λ_i) is defined as

$$\lambda_i = \frac{KK_{ri}}{\mu_i} \tag{2.20}$$

where K is the absolute permeability, K_{ri} is the relative permeability of phase i, and μ_i is the viscosity of phase i.

The mobility ratio (M) is a dimensionless quantity. It affects both areal and vertical sweep, with sweep decreasing as M increases for a given volume of fluid injected (Green and Willhite, 2008), and also affects the stability of a displacement process, with flow becoming unstable when $M > 1.0$. It is called viscous fingering and refers to unfavorable mobility ratio. Contrarily, if $M < 1.0$, it is referred to as a favorable mobility ratio. In this case, under an imposed pressure differential, the oil will be able to travel with a velocity equal to or greater than the velocity of the water.

2.6. CRUDE OIL/ROCK/BRINE INTERACTIONS

The interactions between crude oil, brine, and the reservoir rock are very complex (Jadhunandan and Morrow, 1995). Therefore, it is crucial to study the various components involved in these interactions, in order to understand some of the mechanisms of oil/brine/rock reactions. Oil recovery by waterflooding, including LSWF, is strongly de-

pendent on the interactions between oil, brine, and rock. There is no simple explanation on how these interactions affect recovery by LSWF, and this makes it more important to take into consideration.

2.6.1. Crude Oil. Crude oil is a complex mixture of hydrocarbons and polar organic compounds of oxygen, sulphur, and nitrogen, and it also sometimes contains metal-containing compounds such as vanadium, nickel, iron, and copper (Skauge *et al.*, 1999). Due to the complex composition and different structures, no two oils are exactly the same in their compositions.

Based on the chemical composition, crude oil is divided into four classes: saturates (S), aromatics (A), resins (R), and asphaltanes (A). Figure 2.6 gives examples of the chemical compositions of crude oil.

Saturates are non-polar hydrocarbons, also called paraffins, and they occur as open or straight-chains joined by a single bond. Examples of non-polar hydrocarbons are methane, ethane, propane, and decane. Naphthene are ringed molecules and are also called cycloparaffins. These compounds, like paraffins, are saturated and very stable. They make up a second primary constituent of crude oil. Aromatic hydrocarbons refer to benzene, and structural derivatives such as toluene, naphthalene, and anthracene. These compounds are quite stable, though not as stable as paraffins. Resins are defined as polar-compounds that are soluble in n-pentane, n-hexane, or n-heptane (Demirbas and Taylan, 2016). These compounds contain polar molecules with heteroatoms such as nitrogen, oxygen, and sulfur (Mitchell and Speight, 1973). Asphaltenes are defined as insoluble components in the small liquid hydrocarbons. They are a group of high molecular weight components, with approximately 85% of carbon.

Acids occurring in hydrocarbons have been analyzed, extracted, and tested on many occasions and found to be important due to their interfacial activity (Meredith *et al.*, 2000). There are several factors controlling the amounts of acidic components present in the hydrocarbons. They include the type of sediment that the hydrocarbons are from, how long

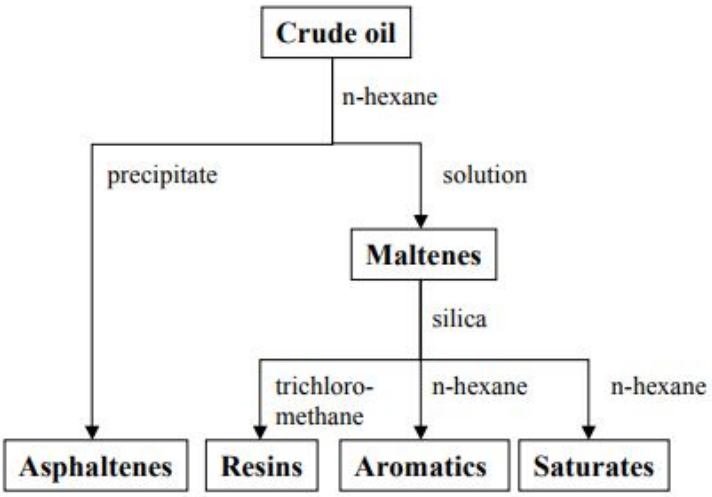

Figure 2.6. SARA-separation scheme (Aske, 2002).

it has been buried, how deep it was buried, and the biodegradation process. In order to assess how acidic a crude oil is, total acid number (TAN) and total base number (TBN) are used. TAN is determined by the amount of potassium hydroxide (KOH) in milligrams that is needed to neutralize the acids in one gram of crude oil, and TBN is a measurement in basicity that is also expressed in the same term as TAN (mgKOH/g oil) (Sorbo, 2016).

2.6.2. Brine. The chemical compositions of both connate brine and injected brine have been shown to have effects on crude oil/brine/rock interactions, wettability, interfacial tension, relative permeability and capillary curves (Jadhunandan and Morrow, 1995). Typical brine compositions that are used for synthetic brines in the laboratory include water, NaCl, Na_2SO_4, KCl, $MgCl_2.6H_2O$, $CaCl_2.2H_2O$, $NaHCO_3$, and $SrCl_2.6H_2O$. These synthetic brines are used as formation water (FW), sea water (SW), and low-salinity water (LSW). Shehata and Nasr-El-Din (2015) stated that the reservoir cores saturated with connate water containing divalent cations of Ca^{2+} and Mg^{2+} showed higher oil recovery than for cores saturated with monovalent cation Na^{+} only.

2.6.3. Sandstone Rock. Sandstone is a type of clastic sedimentary rock, mostly composed of sand-sized minerals or rock grains (Alden, 2017). Sandstones have two different kinds of material (matrix and cement) in it besides the sediment particles. Matrix is the fine-grained material (silt and clay size), that is present within the interstitial pore space between the framework grains. Cement is the mineral matter that binds the siliclastic framework grains together.

Furthermore, Alden (2017) explained that quartz and feldspar are two dominating minerals in sandstone. The other minerals are clays, hematite, ilmenite, amphibole, mica, lithic fragments, biogenetic particles, and heavy minerals. The cement materials are mostly calcite, quartz (silica), clays, and gypsum. The minerals either bind the matrix or fill in the pore spaces.

Clay refers to naturally occurring material composed primarily of fine-grained minerals. Clay is generally plastic when at the appropriate water content and will harden when fired or dried (Guggenheim, 1995). Clays form shale rocks and are a major component in nearly all sediment rocks. The small size of the particles and their unique crystal structures give clay materials special properties, including cation exchange capabilities, plastic behavior when wet, catalytic abilities, swelling behavior, and low permeabilities. The main groups of clay minerals are as follows:

1. Kaolinite group, which includes kaolinite, dickite, nacrite, and halloysite. It is formed by the decomposition of orthoclase feldspar (e.g., in granite).

2. Illite group, which includes hydrous micas, phengite, brammalite, celadonite, and glauconite. It is formed by the decomposition of some micas and feldspars, and is predominant in marine clays and shales.

3. Smectite group, which includes montmorillonite, bentonite, nontronite, hectorite, saponite, and sauconite. It is formed by the alteration of mafic igneous rock rich in calcium and magnesium. A weak linkage by cations (e.g., Na^{+}, Ca^{2+}) results in high swelling and shrinking potential.

4. Glauconite, is an iron potassium phyllosilicate (mica group) mineral with a characteristic green color and very low weathering resistance and is very friable (Odin, 1988). A typical chemical representation of glauconite is (K,Na)(Al, Fe, Mg)$_2$(Al, Si)$_4$O$_{10}$(OH)$_2$. Glauconite can contain high amount of smectite which is an expanding clay mineral when it comes in contact with water (Deer *et al.*, 1992).

5. Vermiculite, is a hydrous phyllosilicate mineral that undergoes expansion when heated. It is formed by weathering or hydrothermal alteration of biotite or phlogopite (Potter, 2000). Its associated mineral phases include corundum, apatite, serpentine, and talc.

The size of clay particles is defined as less than 2 μm in equivalent diameter, whereas the size of migratory fines may be as large as 50 μm (Schulze, 2005). These small particle sizes result in high surface areas, making clay minerals to react readily and rapidly with fluids introduced into a sedimentary rock.

2.7. PROPOSED MECHANISMS OF LSWF

The LSWF studies have been widely accepted by many researchers, institutions, and companies proposing different mechanisms to explain the process. For a long time, several mechanisms have been proposed and many papers have been written on the subject to either support the proposed LSWF mechanisms or to disprove them. While the studies keep increasing each year, there has not been a generally accepted mechanism to explain the process and why LSWF is more advantageous than conventional waterflooding. Thus,

it is safe to take notice all the proposed mechanisms shown here are still widely open to debate. There are ten proposed LSWF mechanisms that are discussed in this thesis, and most of these mechanisms are related to and/or conflicting each other.

2.7.1. Clay Hydration (1967). Bernard (1967) explained that when hydratable clays are present, a fresh waterflooding can produce more oil than brine. The fresh water hydrates the clays and lowers the permeability. The flood water generates a relatively high pressure drop. Clays attract and strongly hold an appreciable amount of water on their surfaces; the less saline the water is, the more of it can be held by the clays. This action and the swelling action, will reduce the effective pore volume, and thereby may affect oil recovery in the waterflooding process.

Engelhardt and Tunn (1955) also investigated that the flow of various fluids through sandstones with clay contents of 1 to 5% shows that the Darcy equation holds for air, carbon tetrachloride, and cyclohexane. In the case of a NaCl solution, the velocity in a given sandstone at a constant pressure drop is higher when the salt concentration is greater. It is assumed that this phenomenon can be explained by the fact that the water becomes bonded to the surface because the clay minerals present in the sandstones by dipole forces and osmotic equilibrium.

Nevertheless, Sohrabi *et al.* (2017) show that the significant additional oil recovery obtained by low-salinity water injection in the clay-free core revealed that the presence of clay is not necessary for LSWF to work. In the inert porous medium, the main mechanism of oil recovery by LSWF was because of the fluid/fluid interactions (microdispersion formation). This statement is also supported by Farzaneh *et al.* (2017), who stated that it was possible to see an improvement in oil displacement by low salinity in clay-free micromodels. This shows that the presence of clay, specifically kaolinite might not be a necessary condition for LSWF to enhance oil recovery as it is described in the previous theory (Boussour *et al.*, 2009). It might be possible that kaolinite reacts faster than other type of clay due to its low cation exchange capacity (CEC).

2.7.2. Fines Migration (1999). Tang and Morrow (1999) proposed that the migration of clay fines might be the main reason for the observed increasing of oil recovery associated with LSWF. They explain that when low-salinity water is injected, the electrical double layer between particles is expanded, and then the tendency of water to remove fines is increased. In contact with low-salinity water, oil-wet clay particles detach from the pore surface, causing an increase of oil mobility. This is also emphasized by Zeinijahromi and Bedrikovetsky (2015), who show that fines mobilization and permeability reduction in swept zones during the low-salinity waterflooding can result the sweep efficiency enhancement. However, Lager *et al.* (2008a) argued that the BP LSWF corefloods showed increased oil recovery with no observations of fine migration or significant permeability reductions.

2.7.3. Alkaline-Flooding Behavior (2005). McGuire *et al.* (2005) proposed that the generation of surfactants from the residual oil at elevated pH levels is a major factor of LSWF mechanism. As low salinity water is injected to the core, hydroxyl ions are generated through reactions with the mineral native to the reservoir and pH is increased about 7 to 8 ranging up to pH 9 or more. The increasing pH causes the process to behave in a similar way to alkaline flooding that reduces IFT between the oil and water, increases the water wettability, and results in higher oil recovery. McGuire *et al.* (2005) also mentioned that low salinity water injected into the reservoir appears to alter the properties of crude oil.

Furthermore, McGuire *et al.* (2005) tried to use the mechanism of alkaline-flooding behavior to explain why not much high recovery was observed in the high-salinity waterflooding process. They explained that in the high-salinity process, the presence of divalent cations (Ca^{2+} and Mg^{2+}) will precipitate the natural surfactants in crude oils and prevent them from increasing oil recovery, whereas, the low-salinity water will always have a low concentration of these divalent cations.

In some studies, it has been reported that a high acid number (TAN>0.2) is needed to generate enough surfactants to reduce wettability reversal and/or emulsion formation. However, there are also reported the cases of improved oil recovery by LSWF with crude

oils with acid number TAN<0.05. Lager *et al.* (2008a) also stated that experiments on the North Slope core sample only showed an increase in pH from 5 to 6 with an increase in oil recovery. They reported that most reservoirs containing CO_2 and H_2S gases will act as a pH buffer, rendering an increase of pH up to 10.

2.7.4. Multicomponent Ionic Exchange-MIE (2006). Lager *et al.* (2008a) reported that multicomponent ion exchange (MIE) occurring between oil, brine, and rock surfaces could be the possible mechanism that causes the increase in oil recovery by LSWF. The theory was applied to enhance oil recovery in the 1970s by Pope *et al.* (1978). The researchers stated that MIE is the basis of geochromatography. It involves the competition of all the ions in pore water for the mineral matrix exchange sites. On an oil-wet surface, multivalent cations on a clay surface will bond to polar compounds present in the oil phase (resin and asphaltenes) forming organo-metallic complexes. At the same time, some organic polar compounds will be adsorbed directly to the mineral surface, thereby enhancing the oil wetness of the clay surface. In relation to low salinity, the MIE mechanism suggests that during the flood, MIE will take place, removing directly adsorbed organic compounds and organo-metallic complexes from the surface and replacing them with uncomplexed cations. This leads to desorption of organic matter, promotes water wetness of the clay surface, and results in improved oil recovery.

Lager *et al.* (2008a) also reported an interesting observation that removing Ca^{2+} and Mg^{2+} from the rock surface before waterflooding led to higher recovery, irrespective of salinity. This is important as they experienced for the first time that no improved oil recovery was observed when low-salinity water was injected into a clastic reservoir where the mineral structure was preserved. Figure 2.7 shows the example of MIE leading to hydrocarbon release.

This MIE mechanism is also supported by Nasralla and Nasr-El-Din (2011), who found that the low-salinity water injection leaches cations from the rock surface, which results in a change of the surface charges of the rock. The low-salinity water generates

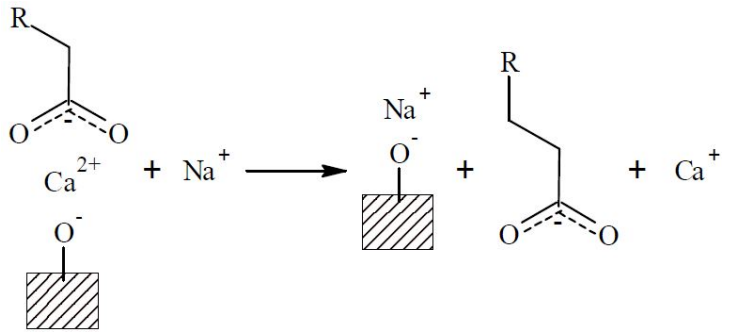

Figure 2.7. An example of multicomponent ion exchange leading to hydrocarbon release (Cotterill, 2014).

repulsion forces, which reduces electrostatic attraction forces between crude oil and the rock surface, and wettability is altered. The effect of cation type on recovery factor (RF) leaches Ca^{2+} from the rock and significantly contributes to oil recovery. As long as the injected brine was $CaCl_2$ free, decreasing the concentration of NaCl in the injected brine did not affect the amount of Ca^{2+} exchange between the brine and the rock.

2.7.5. Salting-in Effect - A Chemical Mechanism (2009). The solubility of polar organic compounds in water is affected by ionic composition and salinity. A decrease in salinity below a critical ionic strength can increase the solubility of organic material in the aqueous phase, which is called the salting-in effect (RezaeiDoust *et al.*, 2009). The salting-in mechanism is a chemical mechanism that is based on the assumption that low salinity effects are linked to improving water wetness of the clay. The adsorbed organic material must be loosely bonded to the surface and be able to be desorbed from the surface due to increased solubility in water.

2.7.6. Electric Double Layer-EDL (2009). Double-layer expansion relies on the observation that a decrease in total salinity is required to observe the LSWF, rather than just a decrease in divalent ion concentration (Ligthelm *et al.*, 2009). The distribution of ions around clay particles forms a double layer, which is an adsorbed layer close to the clay surface and a diffuse layer containing ions that exhibit Brownian motion. During LSWF,

the divalent cations are exchanged for monovalent cations that cannot hold the oil to the surface anymore. The water layer which is adjacent to the surface then thickens as double layer expands as the salinity decreases, driving the clay surface to become more water wet, and thus more oil is recovered. Ashraf *et al.* (2010) also stated that as the salinity of the electrolyte decreases, the thickness of electrical double layer and hence electrostatic repulsiveness increases, which ultimately helps in releasing oil from the pore of the rock surface. Figure 2.8 shows a simple schematic of an electrical double layer.

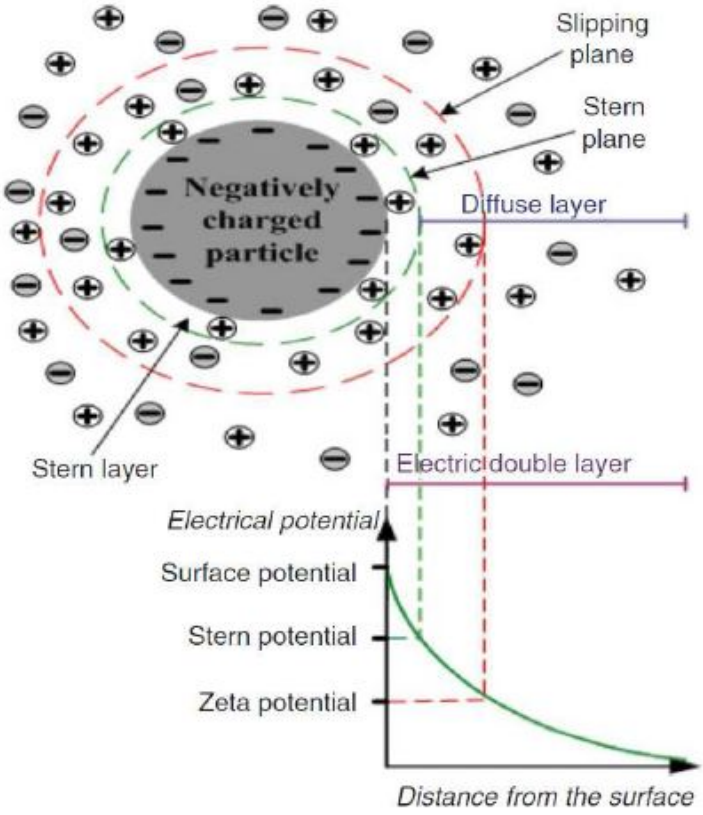

Figure 2.8. A schematic of electrical double layer (Cotterill, 2014).

Nasralla and Nasr-El-Din (2011), Nasralla *et al.* (2011a), Nasralla *et al.* (2011b), and Nasralla and Nasr-El-Din (2012) also conducted studies that support the electrical double layer mechanism. The researchers explained that correlating the zeta potential measurements to coreflooding shows that the electric double-layer expansion, which results from the forces between oil and rock, could be a dominant mechanism in improving oil

recovery by LSWF during secondary recovery mode. Lowering the pH of low-salinity brine changed the electric charges at both oil/brine and rock/brine interfaces from highly negative to close to zero, which decreases the repulsive forces and reduces double-layer expansion, as a result the rock becomes more oil wet and oil recovery is suppressed compared to LSWF at the original pH of the brines.

This EDL mechanism is also supported by Shehata and Nasr-El-Din (2015) who emphasized that the composition of connate water is important. Reservoir cores saturated with connate water containing divalent cations of Ca^{2+} and Mg^{2+} showed higher oil recovery than for cores saturated with monovalent cations of Na^{+}. The ions exchange effect was more pronounced than the pH effect in LSWF. Furthermore, as the temperature increased from 77 to 150°F, an additional oil recovery up to 15.4% OOIP was observed by spontaneous imbibition for Buff Berea cores. The end-point of water relative permeability was also observed to slightly decrease for the cores after using low-salinity brine compared to after injection using high-salinity brine (Shehata *et al.*, 2016).

2.7.7. Mineral Dissolution (2010). Pu *et al.* (2010) carried out a study on recovery of residual oil by LSWF for all tested cores from Tensleep oil zones. Flooding of the Tensleep reservoir cores with sodium chloride solution resulted in production of sulfate ion content of the effluent brine through dissolution of anhydrate cement. The release of domestic crystals and other fine embedded minerals which is likely associated with the dissolution of anhydrate, may be a factor in the observed LSWF.

2.7.8. pH-Induced Wettability Change - A Chemical Mechanism (2010). Another chemical mechanism was also proposed by Austad *et al.* (2010) and supported by Pinerez T. *et al.* (2016). The researchers assumed that at reservoir conditions, the pH of formation water is about 5 due to dissolved acidic gases like CO_2 and H_2S. At this pH, the clay minerals, which act as cation exchange materials, are adsorbed by acidic and protonated basic components from the crude oil and cations, especially divalent cations from the formation water. Injection of low-saline fluid, which promotes desorption of divalent

cations, will create a local increase in pH close to the brine/clay interface because Ca^{2+} is substituted by H^+ from the water. A fast reaction between OH^- and the adsorbed acidic and protonated basic material will cause desorption of organic material from the clay. This improves the water wetness, and an increase of oil recovery is observed. This mechanism is likely to be an extension of the MIE mechanism proposed by Lager *et al.* (2008b) and the salting-in effect mechanism proposed by RezaeiDoust *et al.* (2009).

2.7.9. Water Micro-Dispersions (2013). Emadi and Sohrabi (2013) and Sohrabi *et al.* (2017) reported that when low-salinity brines come in contact with certain crude oils, a large number of water micro-dispersions form at the oil/water interface within the oil phase. The water micro-dispersions do not form when the oil is in contact with high-salinity brine. When the micro-dispersions form due to the low-salinity of the brine, they coalescence as soon as the oil comes in contact with high-salinity brine. The formation of micro-dispersions results in additional oil recovery through two separate mechanisms: (1) depletion of the oil/water interface from natural surface active materials, resulting in wettability alteration, and (2) swelling of droplets of high-saline connate water.

2.7.10. Osmosis - A Novel Hypothesis (2016). A novel hypothesis mechanism based on the osmotic expansion from connate water is proposed by Sandengen *et al.* (2016). The osmosis can occur in an oil/brine/rock system when injecting low-salinity water, because the system is full of an excellent semipermeable membrane, which is the oil itself. This mechanism is supported by Fredriksen *et al.* (2016) who studied water transport and oil mobilization, which was qualitatively observed at pore level, and documented and tracked as a function of time in the presence of a salinity gradient. The transport was identified as water diffusion through film-flow along water-wet grains and osmosis transporting low-salinity water into connate water-in-oil emulsions.

The comprehensive LSWF proposed mechanisms are shown in the Appendix of Summary Table.

2.8. CONDITIONS NECESSARY FOR LSWF AND PARAMETERS AFFECTING ITS PROCESS

Most of the studies conducted on LSWF share common background and support each other, but there are some that disagree with each other. For instance, Alvarado *et al.* (2014) stated that the asphaltenes content of the crude oil is a good qualitative indicator of the ability of the crude oil to form a viscoelastic interface that is needed in the LSWF process. However, Kakati *et al.* (2017) studied that LSWF could be a potential EOR method for light-oil reservoirs with more paraffinic content.

2.8.1. Conditions Necessary for LSWF. Based on the proposed LSWF mechanisms in the previous section, some of the conditions that are necessary for effective application can be summarized below:

1. Clay minerals present in the rock (Bernard (1967); Lager *et al.* (2008a)), but no kaolinite presence is necessary (Boussour *et al.*, 2009), and high CEC clay minerals are favorable (Austad *et al.*, 2010).

2. Presence of connate water (Lager *et al.* (2008a)).

3. Formation brine contains divalent cations (Lager *et al.* (2008a); Ligthelm *et al.* (2009), Austad *et al.* (2010)), with high salinity (Emadi and Sohrabi, 2013).

4. The rock is a intermediate-wet or weakly water-wet system (Emadi and Sohrabi, 2013)

5. Brine injected is Ca^{2+} free (Nasralla and Nasr-El-Din, 2011).

6. Crude oil contains polar components (Alvarado *et al.* (2014); Austad *et al.* (2010)).

7. pH of water is preferentially about 5 (Austad *et al.*, 2010).

The presence of these conditions still does not guarantee the effectiveness of the improved oil recovery by LSWF. The LSWF process is more complex and there is still no single explanation to fully describe its conditions.

2.8.2. Factors Affecting LSWF Process. Most researchers agree that wettability alteration is the dominant mechanism the during LSWF process. Therefore, any conditions that directly or indirectly affect the wettability of a crude oil/brine/rock system will also affect the LSWF process. It has been reported that there are some factors affecting the LSWF process:

1. Influence of crude oil; retention of polar oil components is higher for crude oil with a high base/acid ratio (Skauge *et al.*, 1999). For the crude oil with high acidic components (low base/acid ratio), the retention of polar oil components is affected by the brine composition. Lower salinity gives higher retention of polar oil components. Whereas, for the crude oil with low-acidic components (high base/acid ratio), the retention of polar-oil components was found to not be much affected by the brine composition (Fjelde *et al.*, 2014).

2. Brine composition; the experiments conducted by Shehata and Nasr-El-Din (2015) shows that reservoir cores saturated with connate water containing divalent cations of Ca^{2+} and Mg^{2+} showed higher oil recovery than for cores saturated with monovalent cations of Na^{+}. Nasralla and Nasr-El-Din (2011) also concluded that as long as the injected brine was $CaCl_2$ free, then decreasing the concentration of NaCl in injected brine did not affect the amount of Ca^{2+} exchange between the brine and the rock.

3. Aging temperature; Jadhunandan and Morrow (1995) carried out a study that indicates high aging temperature drives a crude oil/brine/rock system to be more oil wet. Nasralla *et al.* (2011b) also studied the adsorption of oil components on mica surfaces and found that a high aging temperature was associated with a high adsorption of oil components onto mica surfaces.

4. Initial water saturation; the presence of initial water saturation is important in the LSWF process (Lager *et al.*, 2008a). An increase in initial water saturation decreases the adsorption of oil components on rock surfaces.

5. Cation exchange capacity (CEC); cation exchange capacity (CEC) of clay is the ability of clay minerals to exchange cations adsorbed to the naturally negative charged external surfaces and between the layers of the clay structure (Hamilton, 2009). CEC is a measure of the clay's ability to attract and hold cations from a solution. The forces that attract and hold the cations in a solution are electrostatic and Van der Waals forces. Shabib-Asl *et al.* (2015) explain that the reactivity series of the cations on the rock surfaces by LSWF flooding is: $K^+ > Na^+ > Ca^{2+} > Mg^{2+}$.

6. Interaction between ions and mineral surfaces; based on (Lager *et al.*, 2008b), there are four possible interactions between ions and mineral surfaces during LSWF, which include the following: (1) *Cation Exchange* - cations of like charge are exchanged equally between a solid surface such as clay and a solution, such as brines containing various ions; (2) *Ligand Bonding* - the direct bond formation between a multivalent cation and a carboxylate group; (3) *Cation Bridging* - a weak adsorption mechanism and mostly forms between polar functional group and exchangeable cations on the clay surface; (4) *Water Bridging* - the complexation between the water molecule solvating the exchangeable cation and the polar functional group of the organic molecule.

2.9. FIELD APPLICATIONS

Since the LSWF is environmentally safe, many industries have been applying this method in their fields. In the past few years, numerous field tests, pilot projects, and applications of LSWF have been performed in order to improve the recovery. Some of them are discussed below.

2.9.1. Endicott Field, Alaska. The first comprehensive inter-well field trial of LSWF took place in 2008-2009 in BP's offshore Endicott field on the North Slope of Alaska (Seccombe *et al.*, 2010). Endicott has been produced with crestal gas re-injection and peripheral water injection. It was brought on line in 1987. The salinity and hardness of the reservoir water and sea water are approximately equal.

Four single well tests with the saturation change measured using reactive chemical tracer tests (SWCTTs) were undertaken in the Prudhoe Bay and Endicott fields (McGuire *et al.*, 2005). The tests indicated that the incremental oil recovery from LSWF was in the range of 6-12% OOIP. SWCTTs indicated that the residual oil saturation of high-salinity waterflooding was 41% and is reduced to 27% when low-salinity water was used, giving an incremental oil recovery of 15% OOIP which would be lower when areal and vertical sweep effects are accounted for.

The results analysis in the pilot area by LSWF in comparison to the estimated results of continuing high-salinity waterflooding indicate an incremental recovery of 10% OOIP by the start of the high salinity post flush. The previous corefloodings and single well tests showed an incremental recovery of 13% OOIP for a formation with 12% clay content (Seccombe *et al.*, 2010). Overall, this has been a very useful and successful test of LSWF in the field that can be followed by further trials.

2.9.2. Omar Field, Syria. The secondary LSWF analysis in the Omar Field, Syria, operated by Al Furat (a Shell subsidiary), has been reported by Mahani *et al.* (2011). The light-oil (viscosity=0.3 cP) field came on line in 1989 but experienced rapid pressure loss, indicating an absolute lack of aquifer support. Waterflooding used a river water source with a salinity of 500 mg/L (« 100 mg/L bivalent ions) over a period of 10 years (1992-2002). Formation water salinity is 90,000 mg/L with a high content of bivalent ions (5000 mg/L), and the clay content is 0.5-4% of which 95% is kaolinite.

Special core analysis and coreflooding experiments showed that the native state wettability in Omar field was oil wet, and the average rock permeability was 42 mD. The Al Furat (and Shell) view is that the measurements and observations at 21 wells in the Omar field present proof of wettability alteration during LSWF at the reservoir scale. The analysis indicates that the wettability change is probably from 0.8 or 1.0 to 0.2 which would give an expected incremental oil recovery of 17% OOIP, compared to high-salinity waterflooding. The interpretation is that in this field, viscous forces provide the dominant drive mechanism, which is favorable for the LSWF process. However, the comparison of high- and low-salinity waterflooding across Al Furat's assets shows that a more conservative estimate would be an increase of 5-15% STOIIP from LSWF in Omar field.

2.9.3. Sijan Field, Syria. The low-salinity waterflooding that has been performed in Sijan Field, Syiria is operated by Al Furat (a Shell subsidiary), as a tertiary flooding. Sijan has a very high-salinity formation water (TDS in excess of 200,000 ppm), low connate water saturation, thought to be oil-wet, and rock permeability of 1000 mD (Mahani *et al.*, 2011). In 2005, after re-injecting produced water for more than 10 years, low-salinity injection was started with TDS of less than 500 ppm, in one of the main producing blocks in this field.

Mahani *et al.* (2011) reported that the LSWF in tertiary mode in the Sijan block response has not been identified clearly. There are two important factors that were expected to significantly reduce the benefits of LSWF. First, the presence of a strong buoyancy force caused by the high permeability of rock (significantly larger than the viscous force and much larger than the capillary force) is expected to lead to a partially segregated flow and significantly decrease the additional recovery factor due to LSWF. Second, due to the very high contrast in salinities, injecting large amounts of low-salinity water in the high-salinity formation water leads to a significant decrease in LSWF efficiency.

2.9.4. Burgan Field, Kuwait. The greater Burgan field in Kuwait is the second largest field in the world and the largest clastic reservoir. The Burgan field has been on stream for 66 years under primary production from natural water drive, which is operated by KOC (Abdulla *et al.*, 2013). The KOC has taken a bold step for the first time to do LSWF field trials without extensive laboratory screening. The LSWF trial injection was performed into two producers and comparisons on S_{orw} are made of LSWF versus high-salinity-produced waterflooding. Single well tracers were used to measure the S_{orw}. Furthermore, Abdulla *et al.* (2013) reported the analysis results from this trial, which are as follows:

1. The LSWF was able to reduce S_{orw} by at least 3 s.u. (23.7% of remaining oil after effluent waterflood) in the best quality rock with the least clay content in Burgan, which would still be sufficient to make it economically attractive.

2. There was no damage observed in the injectivity of the wells for the relatively low-clay rich zone, when reducing salinity from 140,000 ppm to 5,000 ppm.

3. Additional tests are planned for the remaining rock types in Burgan that have a higher clay content and the potential for a larger change in oil saturation.

2.9.5. West and North Africa fields. An onshore field in West Africa was the first field selected for EOR study and deployment by Eni (Rotondi *et al.*, 2014). The first tertiary coreflooding tests with low-salinity water were performed in 2007. The first log-inject-log and single well chemical tracer tests to evaluate low-salinity water efficiency at field scale were performed in 2008 and in 2013, respectively. Eni itself has developed an internal workflow and screening criteria for the LSWF process.

The selected field matches with the Eni LSWF screening criteria, which include sandstone rock with high-clay content, oil containing polar components, and formation brine containing divalent ions. The reservoir is heavily faulted and highly heterogeneous due to a complex structural and stratigraphical setting. The fluid is light-crude oil (39° API). Low-salinity water between 1000 mg/L and 5000 mg/L and surfactant injection were

tested in this field as EOR techniques. However, the SWCTT results showed no clear effect of LSWF despite the good indications from laboratory corefloodings, while the surfactant flooding showed very good results.

Rotondi *et al.* (2014) also reported that Eni then implemented such EOR techniques as the combination of LSWF and polymer in order to improve the mobility ratio during waterflooding and increase oil recovery. A giant onshore brownfield in North Africa was selected for this application. The field is characterized by 12 separate sandstone reservoirs with interbedded shales and anhydrite intercalations ranging from the lower to upper Miocene Age. The reservoir fluid is a 20° API gravity oil with viscosity between 6-8 cP at reservoir conditions. In this field, the LSWF was experimentally investigated and was found to provide additional oil recovery of about 7%.

2.9.6. Bastrykskoye Field, Russia. Zeinijahromi *et al.* (2015) carried out a case study of 25 years of LSWF in Bastrykskoye field, Russia. This field consists of two sandstone layers: Tula as the upper layer and Bobrik as the lower layer. The layers are separated by a 6 m impermeable clay. The Tula and Bobrik layers have initial oil saturations of 0.83 and 0.86 with an oil viscosity of 12.6 and 6.8 cP, respectively. The reservoir is connected to an active aquifer, which provides the primary energy of production.

The production from Bastrykskoye field commenced in 1982, and low-salinity water injection started in 1988 to maintain reservoir pressure. The injected water has a significantly lower salinity compared to the formation water, which is 0.2 mol/lit, while the formation water salinity is 4.6 mol/lit. The very high salinity of the formation water is defined by the high sodium chlorite concentration, while the magnesium and calcium concentrations are dominant dissolved salts in the injected low-salinity water. In this case, a large ion exchange is expected to occur during the displacement of the formation water by LSWF.

Furthermore, Zeinijahromi *et al.* (2015) reported that the comparative study of two scenarios of LSW and formation water injection in the Bastrykskoye field shows an insignificant incremental recovery from LSWF, which is the final RF of LSWF and the formation waters are 50.6% and 48%, respectively. This could be explained by a large volume of high-salinity water that has been produced before the start of LSWF.

2.9.7. West Salym Field, West Siberia. Erke *et al.* (2016) reported the field trial of LSWF in the West Salym field, located in West Siberia. The field went on stream in 2004 and conventional waterflooding started in 2005. The West Salym field was considered for deployment of LSWF due to the availability of low-salinity brines from a number of sources, good integration between LSWF and existing waterflooding infrastructure, and also some other factors. Due to insignificant volumes of high-salinity water that was already injected in this field, it was assumed that LSWF would be in the secondary mode. The salinity of injected water was in range of 1500-3000 ppm, which was prepared by mixing fresh water from an aquifer and high-salinity water from a produced water reinjection system. The dynamic reservoir modeling using low salinity permeability curves showed that the LSWF leads to increased oil production up to 2.5% STOIIP. This result establishes the fundamentals of a LSWF field trial in this field.

2.9.8. El-Morgan Field, Egypt. The El-Morgan field was discovered in February of 1965 and is operated by GUPCO (Noureldien and Nabil, 2016). The two oil productive zones were found, Belayim and Kareem formations. The Kareem reservoir is the most significant oil reservoir containing approximately 89% of the total STOIIP for these two combined reservoirs. The reservoir is medium-coarse grained with poorly sorted arkosic sands interbedded with laminated shales.

In appraising the $LoSal^{TM}$ technique, a BP low-salinity water trademark, GUPCO conducted laboratory core experiments, and the results showed a reduction in S_{or} of two saturation unit. In general, $LoSal^{TM}$ showed an improvement in the recovery factor ranging

from 21% from core flood tests up to 54% from single well chemical tracer tests (SWCTT). At the reservoir scale, GUPCO successfully obtained the $LoSal^{TM}$ incremental prize with its uncertainty.

2.9.9. Pervomaiskoye Field, Russia. The Pervomaiskoye oil field in the Republic of Tatarstan, Russia is a field that uses fresh water in its waterflooding projects because of the deficiency of produced water at the initial stage. This field is operated by PJSC TATNEFT. Produced high-salinity water was injected in the wells for more than 25 years, low-salinity water was used for the flooding in 2005. Akhmetgareev and Khisamov (2016) carried out a study of the LSWF effect in this field. They compared the incremental oil production from LSWF versus conventional waterflooding by high-salinity water. The TDS of injected water of high-salinity water and low-salinity water were 252,738 ppm and 848 ppm, respectively. Core laboratory experiments and 3D modeling were performed in this study. The 3D modeling showed that cumulative additional oil production due to LSWF in this field is 4.2 million m3 and the incremental oil recovery is 3.5%. The effect was prominent in wells with water cut from 20% to 90%.

2.9.10. Powder River Basin, Wyoming, USA. According to Robertson (2007) and Thyne and Siyambalagoda Gamage (2011), in the Minnelusa formation in the Powder River basin of Wyoming, numerous fields have been flooded with water from low-salinity sources. The Minnelusa sandstone formation consists of 130 fields with a cumulative production of more than 600,000,000 barrels of oil. There are 55 fields that are flooded with low-salinity water, 52 fields are flooded with mixed-salinity water, and 23 fields are flooded with formation brine. The low-salinity water was derived from wells in the shallow Lance and Fox Hills formation with an average salinity of 2,100 ppm, while the Minnelusa fields had an initial formation salinity ranging from 1,134 to 21,000 ppm. Thyne and Siyambalagoda Gamage (2011) reported that there was no difference in performance as measured by recovery factors and water breakthrough for the Minnelusa fields with low-salinity injection (50.8% OOIP) compared to fields with saline water injection (51.4%

OOIP). It may be because the injected salinity was very similar to the formation water salinity, lack of mobile fines, the inherent properties of the Minnelusa brine-oil-rock system, or the difference in performance was not apparent due to large range of natural variability in recovery.

2.10. LSWF BENEFITS

It is reported in many studies that the injection of low-salinity water into reservoirs has some benefits compared to conventional waterflooding and other EOR techniques. Some of the benefits are as follows:

1. Mitigation of reservoir scaling and souring risks.
2. Injectivity is improved due to lower suspended solids content and corrosivity being reduced.
3. Being a natural extension of waterflooding, the process may be integrated in a conventional water injection plant.
4. It is easier to implement and has lower capital and operational cost than alternative EOR techniques.
5. An alternative technique for water production control (Huff n Puff with low-salinity water).
6. Provision of a low-salinity waterflooding in a field can act as a pioneer for other water based EOR methods such as polymer flooding, alkaline/surfactant/polymer flooding, and linked-polymer system (LPS) with the potential for even greater incremental recoveries.

3. DATA COLLECTION

This thesis carries out a study of low salinity waterflooding in sandstone reservoirs based on laboratory corefloodings and field applications data. The data were collected from 50 literatures for coreflooding between the published year of 1955 and 2017, whereas for field applications, the data were collected from 10 literatures since the published year of 2010 to 2016. The keywords for the data collection are sandstone, low salinity, low salinity waterflooding, low salinity water injection, low salinity effect, coreflooding, and low salinity field. No limitation with regards to the publication date of the references were published. This data collection was performed in August-December 2017.

3.1. COREFLOODINGS DATA SET

There are 471 laboratory experiments data that were collected from 50 literatures. The data set comprises corefloodings and some spontaneous imbibition tests. The data sources are from SPE conference paper, SPE journal paper, Elsevier journal paper, books, and technical reports. A summary of parameters count collected in the database is presented in Table 3.1. It is necessary to be noted that the secondary and tertiary LSWF stage are recorded in this work to analyze effects of some parameters in the secondary and additional tertiary recovery.

Some parameters from laboratory experiments have large numbers of missing values, such as pH rock/brine, core aging times, total acid and base numbers, due to partially unrecorded laboratory observation or unpublished data set. Therefore, this work only analyzes the available data and the missing data are neglected intentionally.

Table 3.1. Summary of collected parameters and their availability.

Parameter	Data Available	% of Missing Data
Core Length (cm)	427	9%
Core Diameter (cm)	412	12%
Porosity (%)	437	7%
Permeability (mD)	399	15%
Initial Water Saturation (%)	306	35%
Sandstone Type	471	0
Total Clay Content (wt%)	116	75%
Kaolinite Content (wt%)	154	67%
pH Rock/Brine	56	88%
Core Aging Temperature (°C)	388	18%
Core Aging Time (days)	258	45%
Wettability Index (IAH)	82	83%
Formation Brine Salinity (ppm)	435	8%
Formation Brine Divalent Ions (ppm)	412	13%
Secondary Injected Brine (ppm)	434	8%
Tertiary Injected Brine (ppm)	159	66%
Injected Brine Divalent Ions (ppm)	395	16%
pH Brine	86	82%
Injected Brine Composition	429	9%
Oil Viscosity (cP)	377	20%
Oil Density (g/cm^3)	348	26%
pH Oil/Brine	86	82%
Oil n-C6 Asphaltenes (wt%)	135	71%
Total Acid Number (mgKOH/ g oil)	168	64%
Total Base Number (mgKOH/ g oil)	148	69%
Test Temperature (°C)	391	17%
Test Pressure (psi)	165	65%
Flow/Injection Rate (ml/min)	379	20%
Secondary Recovery (%OOIP)	375	20%
Additional Tertiary Recovery (%OOIP)	158	67%
Final Recovery (%OOIP)	382	19%
S_{or} (%)	105	78%
Pressure Drop (psi)	67	86%
Secondary/Tertiary LSWF Stage	434	8%

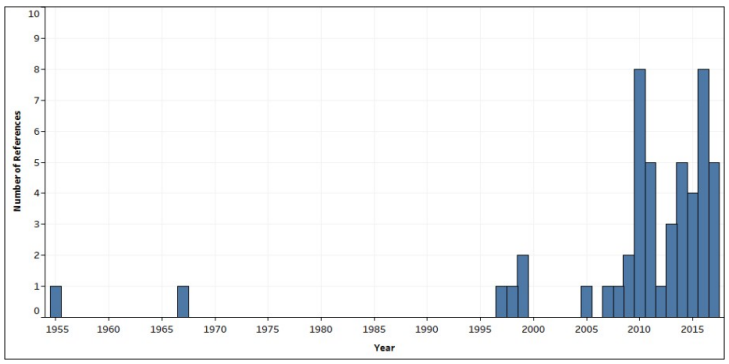

Figure 3.1. Number of references for lab experiments by year.

Data diversity and representativeness are also considered in this work. To avoid inaccurate and bias results, the data were collected as much as it can and mainly for the field application cases, the data were collected worldwide. Figure 3.1 shows the number of references by year for laboratory experiments.

3.2. DATA CLEANING

In the data collection, there are 35 spontaneous imbibition tests and 10 experiments that use micromodels, instead of cores. These 45 tests usually were conducted to gain the wettability index values and observe the clay-free rock. In this analysis, those kinds of data are excluded in order to have uniform criteria. There is no duplication in the data collected to ensure the quality of the results.

Units of the parameters that come from different references were made uniformly, such as core length, core diameter, age temperature, and injection flow rates. In addition, the permeability values that have large range are then divided into three categories, which are absolute permeability, air permeability, and brine permeability.

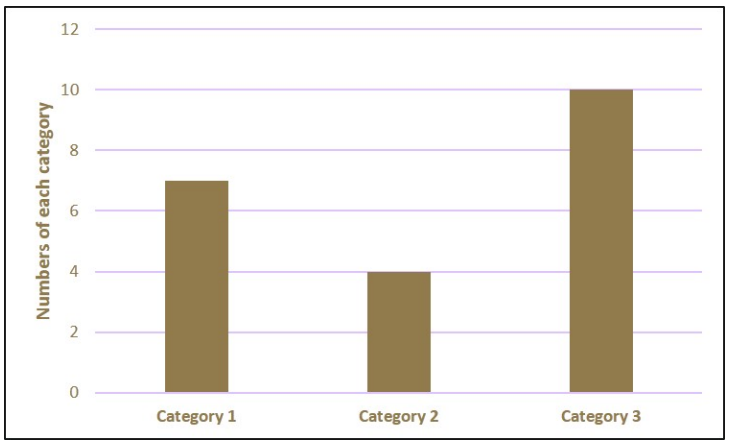

Figure 3.2. An example of a bar chart.

3.3. DATA VISUALIZATION

Some statistical analysis tools are used to visualize and analyze the data, which are bar chart, histogram, boxplot, and cross plot. The plots are generated using MS Excel and Tableau software. A bar chart is used to present caterogical data with rectangular bars, with height or length is proportional to the represented values. A histogram is used to present the distribution of a given variable by depicting the frequencies of observations occurring in certain ranges of values. It used bins to group the values in certain ranges. A boxplot is used to display the full range of data variation from minimum (lower limit) to maximum (upper limit), the likely range of variation (interquartile range/IQR), and the median. A cross plot is used to display of a set of two variables to give good visualization of the relationship between each other. It is also used to detect the special cases. The examples of each tool are shown in Figure 3.2, 3.3, 3.4, and 3.5.

3.3.1. Core Properties. Figure 3.6 illustrates the data set distribution of each sandstone type that are used in the coreflooding experiments and their average permeability. The types of permeability (absolute, air, and/or brine permeability) for each type of sandstones were converted to absolute permeability to make the data set uniform.

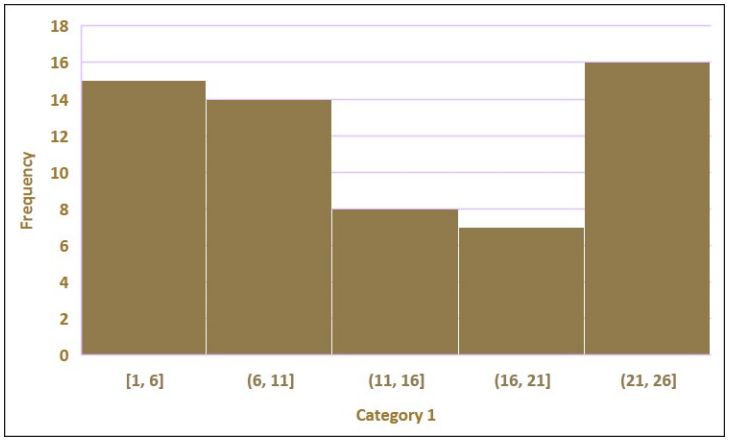

Figure 3.3. An example of a histogram.

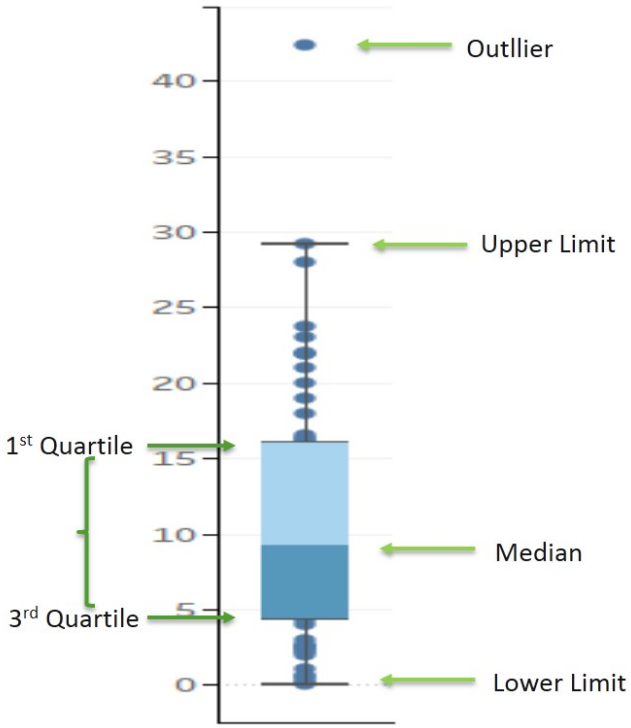

Figure 3.4. An example of a boxplot.

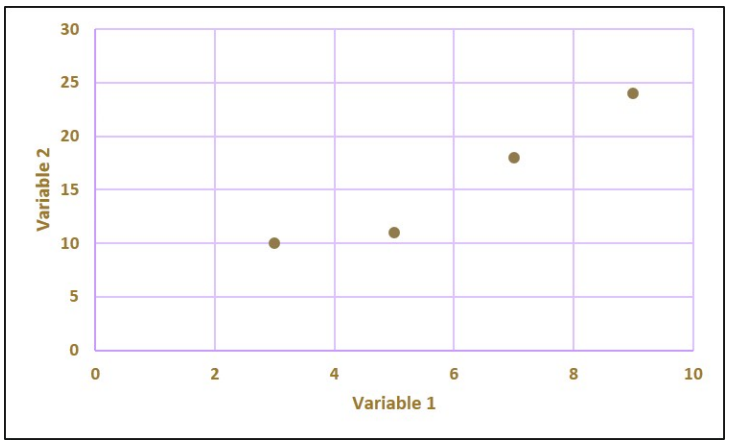

Figure 3.5. An example of a cross plot.

There are 29 types of different sandstone cores and 1 is unknown. The cores from outcrop sandstone are highlighted in red. The highest number of sandstone type that were used in the coreflooding experiments is Berea sandstone, which is 233 data. The Berea sandstone is a sedimentary rock that has predominantly sand-sized grains and are composed of quartz and silica. It has relatively high porosity and permeability, thus those make it a good reservoir rock. The Berea core samples have also been widely recognized as the best stone for testing the efficiency of chemical surfactants.

Core lengths and diameters of coreflooding experiments data are depicted in Figure 3.7. Most of the cores that were used for the corefloodings are 7.8 cm (3 in) in length and 3.81 cm (1.5 in) in diameter. There are some cores that have larger sizes up to 50.8 cm in length and 7.8 cm in diameter, that come from combined cores to achieve certain porosity and permeability.

Core porosity and permeability in the data distribution are illustrated in Figure 3.8 and 3.9, respectively. The corefloodings mostly used the core with porosity 18-24%, which are typical porosity values of the Berea sandstones. The minimum porosity is 5.1% that comes from a core in West Africa sandstone, and the maximum porosity is 40.3% which is a core from North Sea sandstone. The permeability data ranges from 0.3 to 5,570 mD. The

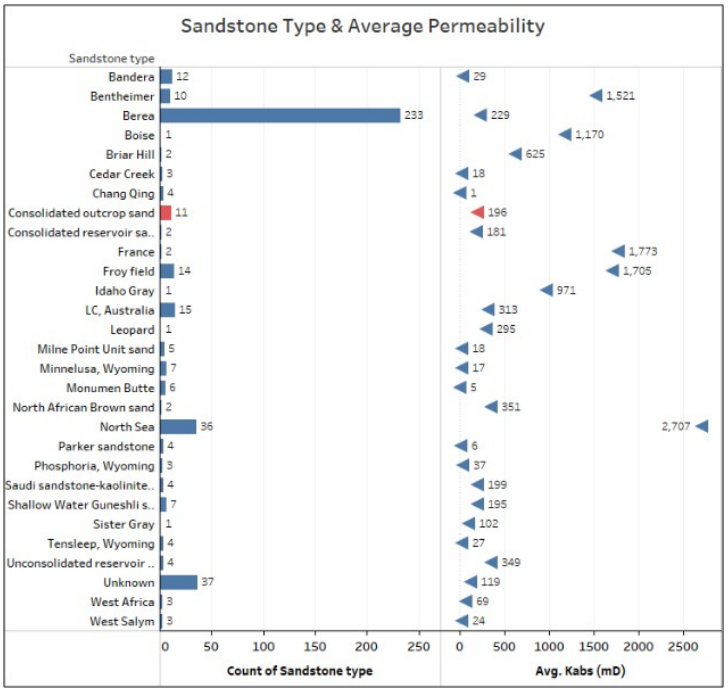

Figure 3.6. The number of each sandstone types and its average permeability.

minimum of 0.3 mD permeability comes from a core in Chang Qing sandstone in China, and the highest value of 5,570 mD comes from North Sea sandstone. The crossplot between porosity and average permeability is shown in Figure 3.10. The data points highlighted in red are cores from outcrop sandstone.

The distribution of initial water saturation data is depicted in Figure 3.11. Most of the frequency value is 29% of S_{wi}. However, there are some high initial water saturation values above 40%, with the highest is 52% of S_{wi} that comes from a low porosity and permeability core in West Africa. The lowest S_{wi} value is 8.1% also comes from a low porosity sandstone in Minnelusa, Wyoming.

3.3.2. Oil Properties. The oil properties that were used for the coreflooding experiments are described in term of viscosity and density. Figure 3.12 shows the distribution of oil viscosity in the data set. Most of the corefloodings used oil with viscosity between 3.5

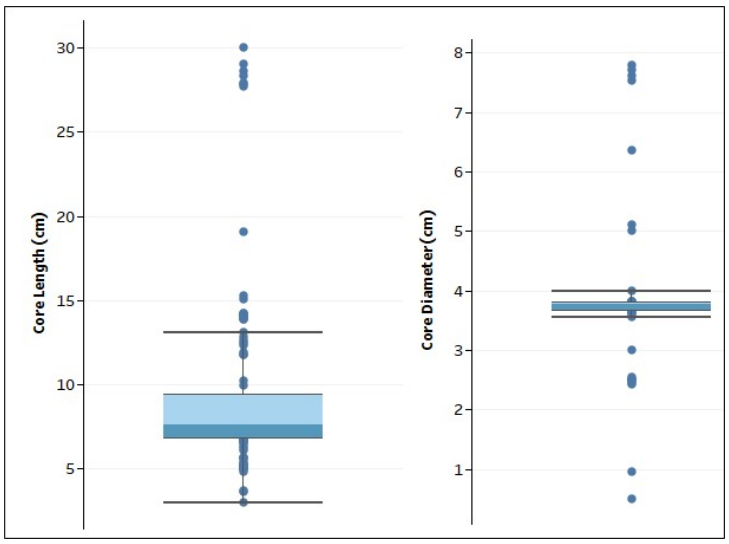

Figure 3.7. Boxplots of core length and diameters.

to 20.4 cP. The heaviest oil that was used is at viscosity of 180 cP from Kuwait medium heavy oil, that also has high asphaltenes and resin content of 17.8%. The lightest oil is at viscosity of 0.3 cP from North Sea.

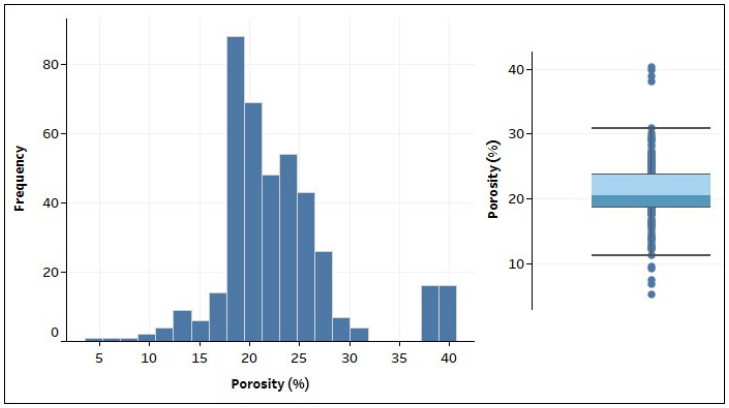

Figure 3.8. Histogram and boxplot of core porosity.

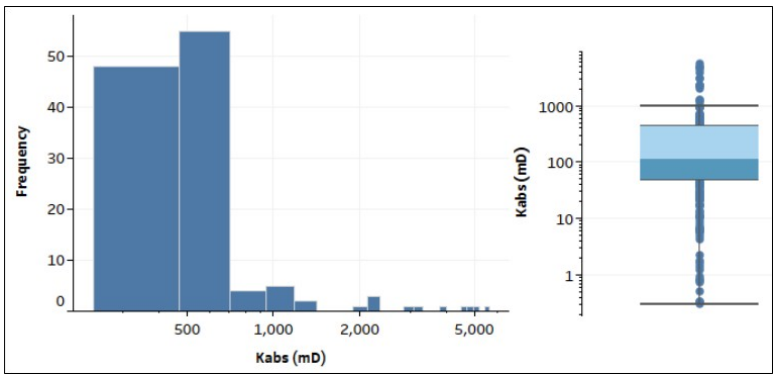

Figure 3.9. Histogram and boxplot of core permeability (Kabs).

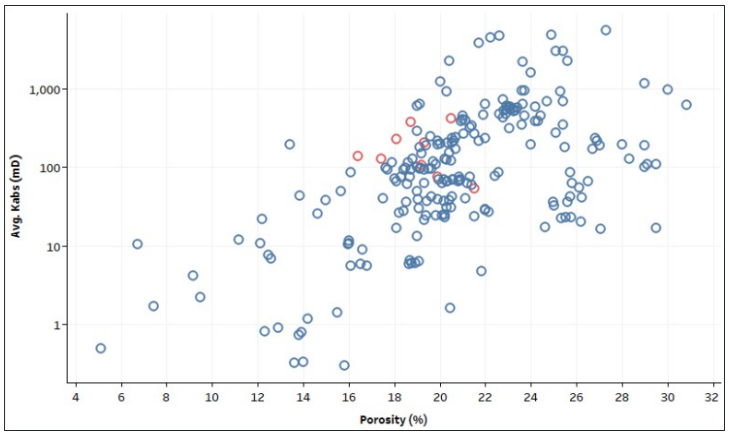

Figure 3.10. Crossplot of average core permeability vs. core porosity.

The crossplot in Figure 3.13 indicates the relationship between oil density and viscosity. There is one data that lies from the majority of the data set (circled in red), which is the lightest oil with viscosity of 0.3 cP and density of 0.65 g/cm^3 coming from North Sea.

In visualizing how acidic the crude oil that are used in the coreflooding experiments is, the boxplots of total acid number (TAN) and total base number (TBN) are depicted in Figure 3.14. Most of the crude oil in the experiments have low acidity which is shown in the boxplots that TAN values range between 0.01 and 1.8 mgKOH/g oil, while the TBN values range from 0.5 to 5 mgKOH/g oil.

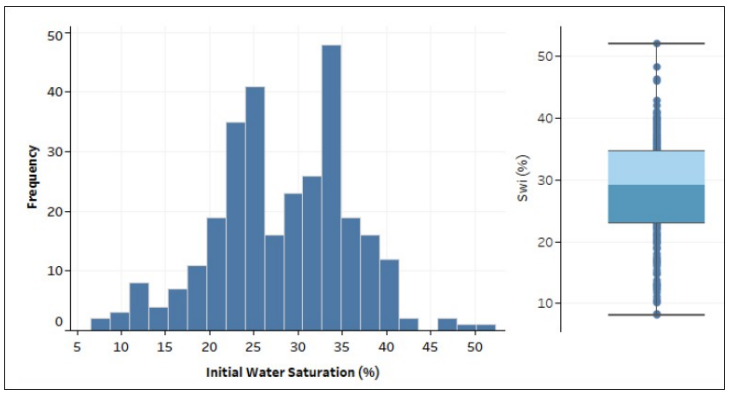

Figure 3.11. Histogram and boxplot of initial water saturation.

The asphaltenes content in the crude oil is also shown in Figure 3.15. It indicates that most of the asphaltenes content distribution in data set is ranging from 1.2 to 6.3 wt%. It has the lowest and highest value of 0 and 10.4 wt%, respectively.

3.3.3. Brine Properties. The formation and injected LSWF brines properties are described here in term of their salinities. The divalent ions concentration in ppm for both formation and injected brines are also illustrated here. Figure 3.16 shows the distribution of formation brine salinity and the divalent ions concentration in the data set. The majority of the formation brine salinity data points fall between 15,150 to 48,202 ppm and the divalent ions concentration data points fall between 227 to 5,850 ppm. It also can be said that the divalent ions concentrations are about 4 to 19% of the formation brine.

Figure 3.17 shows the distribution of injected LSWF brine salinity and the divalent ions concentration in the data set. The data shown here include injected brines for LSWF secondary and tertiary mode. The distribution of the injected brines salinity mostly is between 388 and 3,166 ppm for secondary mode, and 700 to 3,370 ppm for tertiary mode. The divalent ion concentrations in the injected brine are mostly between the values of 45 to 277 ppm for secondary mode, and 53 to 269 ppm for tertiary mode. The lowest value of 0 indicates that the injected brines only content monovalent ions.

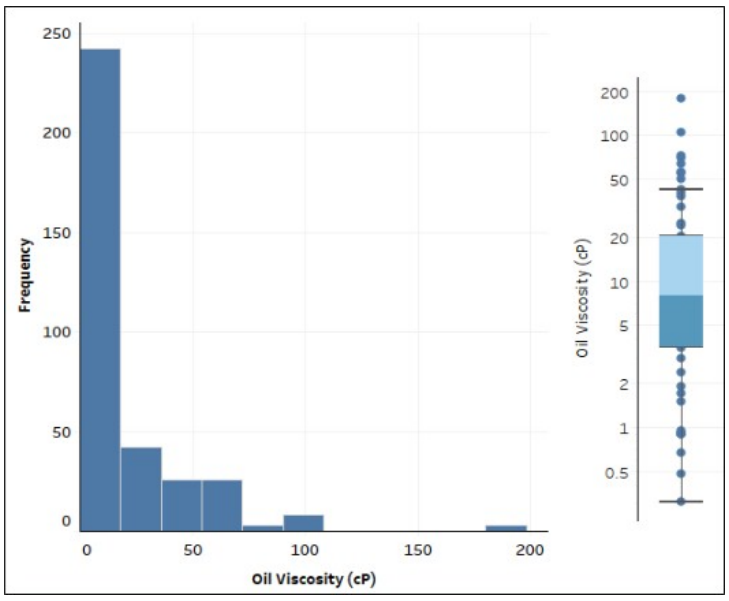

Figure 3.12. Histogram and boxplot of oil viscosity.

Figure 3.18 and 3.19 depict the relationship of formation brine and injected brine salinities in secondary and tertiary LSWF modes, respectively. It can be observed that in the secondary LSWF mode, the coreflooding experiments did not use the formation brine salinity between 60,000 to 100,000 ppm and 130,000 to 170,000 ppm, with the maximum formation brine salinity value is 197,451 ppm. The injected secondary LSWF brine salinity that was used ranges from 106 to 6,836 ppm. In the tertiary LSWF mode, it shows that the coreflooding experiments did not use the formation brine salinity between 70,000 to 100,000 ppm and 100,000 to 170,000 ppm, with the maximum formation brine salinity value is 250,000 ppm. The injected tertiary LSWF brine salinity that was used ranges from 109 to 6,836 ppm.

The ratio of conventional (high-salinity) and the low-salinity waterflooding is used to represent how many times the high-salinity brine is reduced or diluted to get the low-salinity brine for LSWF, and it is called as HS/LS Ratio. It can be expressed mathematically

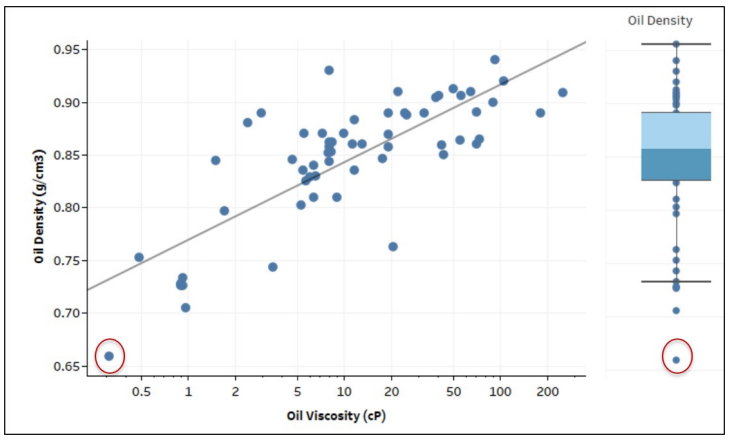

Figure 3.13. Oil density vs. oil viscosity crossplot and boxplot of oil density.

as follow:

$$HS/LSRatio = \frac{Conventional\ water flooding\ salinity\ (ppm)}{LSWF\ brine\ salinity\ (ppm)}. \tag{3.1}$$

The HS/LS ratio both in secondary and tertiary LSWF stages are shown in Figure 3.20. In the secondary LSWF stage, the HS/LS ratio mostly is between 10 to 55. It means the low-salinity brine that is injected in the secondary LSWF stage, comes from between 10 and 55 times diluted high-salinity brine. Whereas, in the tertiary LSWF stage, the injection of low-salinity brine comes from high salinity brine that was diluted between 20 to 83 times. The HS/LS ratio in the tertiary LSWF stage has wider range up to 503, while the ratio in the secondary stage is only up to 244.

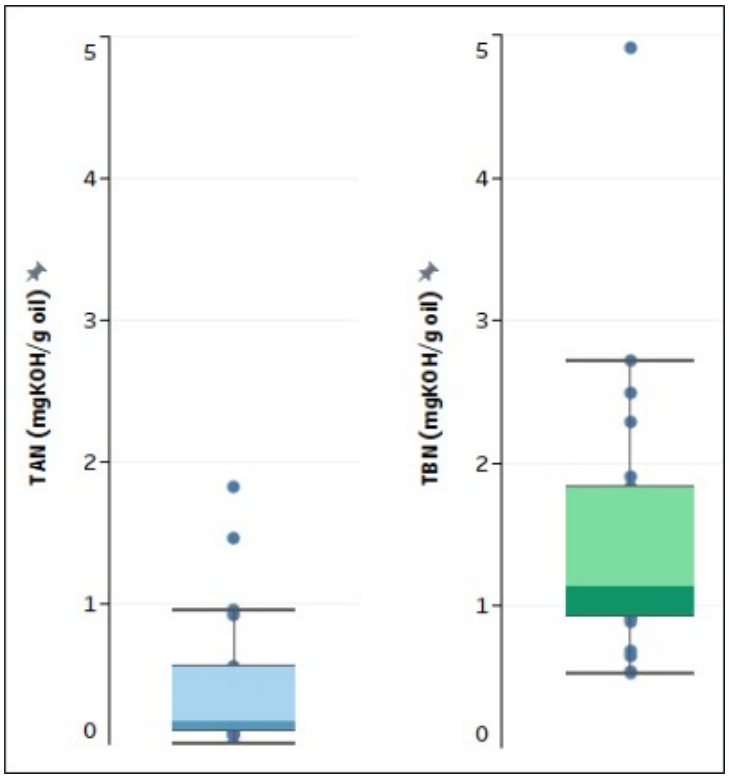

Figure 3.14. Boxplots of the crude oil TAN and TBN.

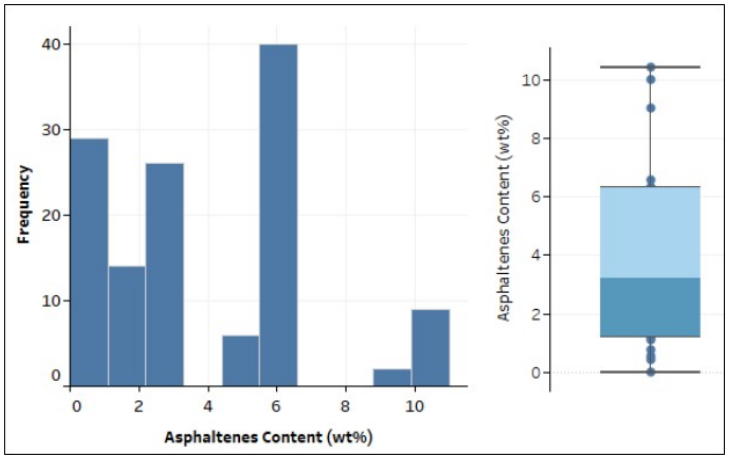

Figure 3.15. Histogram and boxplot of oil asphaltenes content.

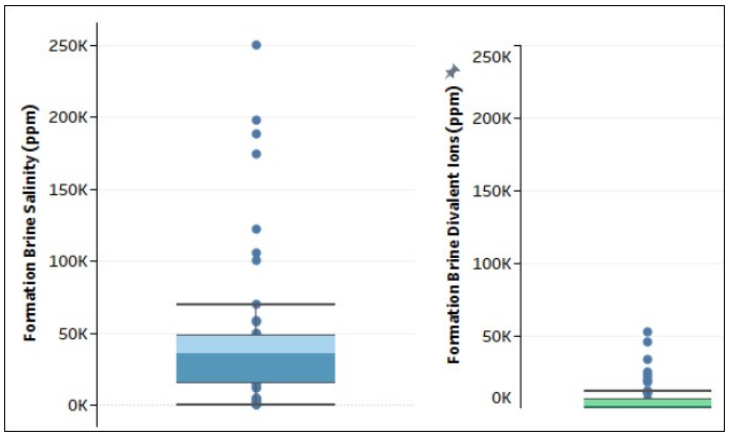

Figure 3.16. Boxplots of formation brine salinity and divalent ions concentration.

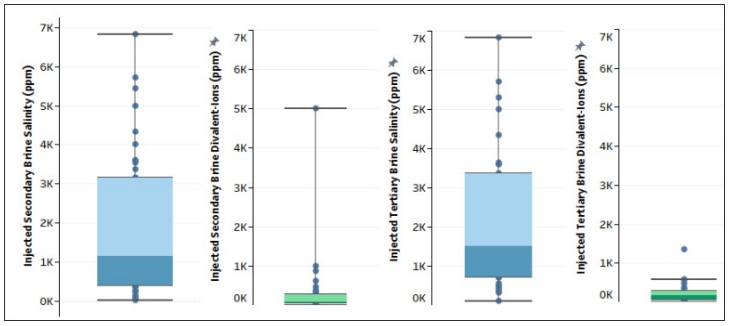

Figure 3.17. Boxplots of injected LSWF brine salinity and divalent ions concentration.

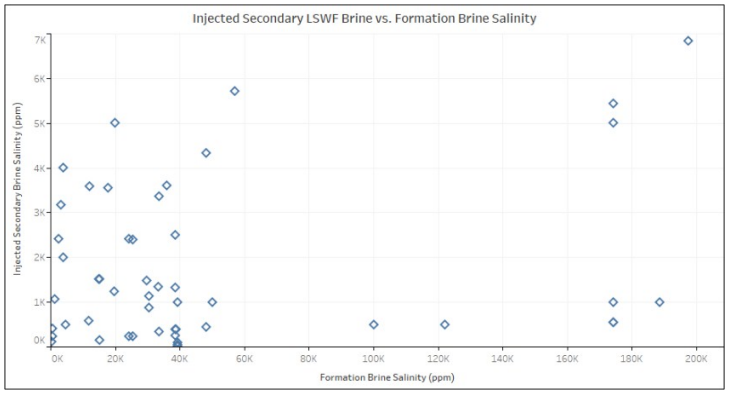

Figure 3.18. The relationship between formation and injected brine salinity in secondary LSWF mode.

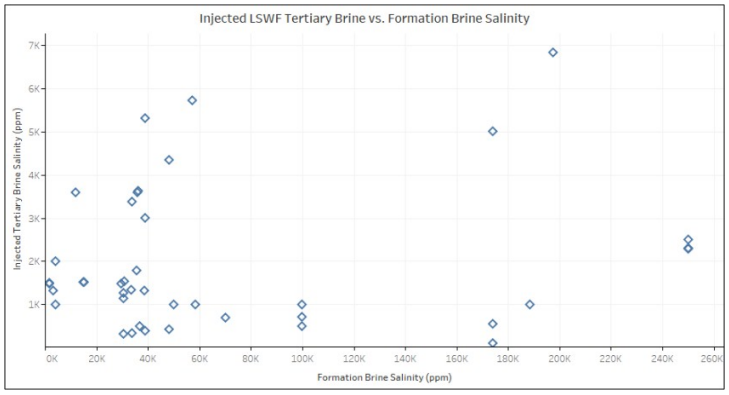

Figure 3.19. The relationship between formation and injected brine salinity in tertiary LSWF mode.

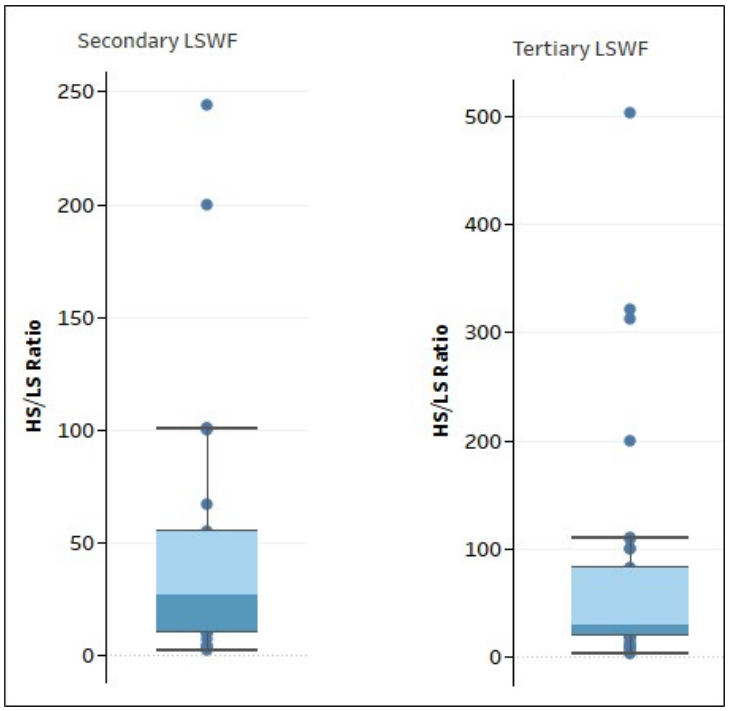

Figure 3.20. Histograms of HS/LS ratio in secondary and tertiary LSWF mode.

4. RESULTS AND DISCUSSION

The important parameters in the coreflooding dataset are taken into account in the oil recovery. In the case of LSWF is in secondary mode, the incremental secondary recovery is calculated as the difference between oil recovery from LSWF and coventional waterflooding (conv. WF). It can be expressed mathematically below:

$$Incremental\ Secondary\ Recovery\ =\ Oil\ Recovery_{secondary\ LSWF} - Oil\ Recovery_{conv.\ WF} \tag{4.1}$$

While, for tertiary LSWF mode, the oil recovery in the data set is the additional recovery after secondary normal waterflooding. There are also some corefloodings that did the LSWF in both secondary and tertiary mode (secondary+tertiary). In this case, the oil recovery values that were obtained from the secondary mode, are compared to the values from normal (high salinity) waterflooding from the most similar core and oil properties in the same reference. Furthermore, the additional recovery values from tertiary LSWF mode are included in the tertiary recovery analysis.

4.1. EFFECT OF ROCK POROSITY AND PERMEABILITY ON OIL RECOVERY

The effect of rock properties in term of porosity and permeability are analyzed in the secondary and tertiary LSWF modes.

4.1.1. Secondary Mode. Figure 4.1 shows the relationship of both porosity and permeability to the incremental oil recovery in the secondary LSWF mode. Most of the data show the incremental oil recovery between 4 to 16% OOIP, regardless the porosity and permeability values. The highest incremental recovery (pointed by black arrow) is 42% OOIP from the Berea core that has porosity and K_{abs} of 20.33% and 351.8 mD, respectively. The coreflooding with this core used the formation brine that does not contain

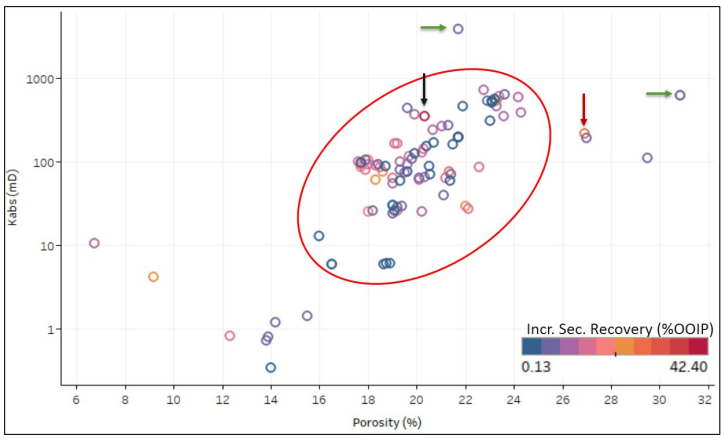

Figure 4.1. Porosity-permeability relationship to the incremental secondary recovery.

divalent ions (Ca^{2+} and Mg^{2+}). This is a counter-evidence of the multicomponent ionic exchange (MIE) and electric double-layer (EDL) mechanisms that state the formation brine must contain divalent ions. Production of fines was found during inspection of effluent samples (Alvarado *et al.*, 2014). This evidence supports the fines migration mechannism. It also used the crude oil with 5 wt% asphaltenes content that is a good indicator of the ability of the crude oil to form a viscoelastic interface. The other core with porosity of 26.9% and K_{abs} of 655 mD also yields high incremental oil recovery which is 29.2% OOIP (pointed by red arrow). The coreflooding with this kind of core from LC, Australia, was using formation brine with salinity of 29,690 ppm that contains 1,012 ppm of divalent ions (Ca^{2+} and Mg^{2+}). It also used the crude oil that contains 3.2 wt% asphaltenes content (Zhang *et al.*, 2007). The highest porosity and the highest permeability cores (pointed by green arrows) give incremental secondary recovery of 5% and 7.4% OOIP, respectively.

The data that yield incremental secondary recovery mostly have porosity of 18-24%, and permeability of 40-500 mD, as circled in red. The detail distribution of porosity and permeability are shown in Figure 4.2 and 4.3, respectively.

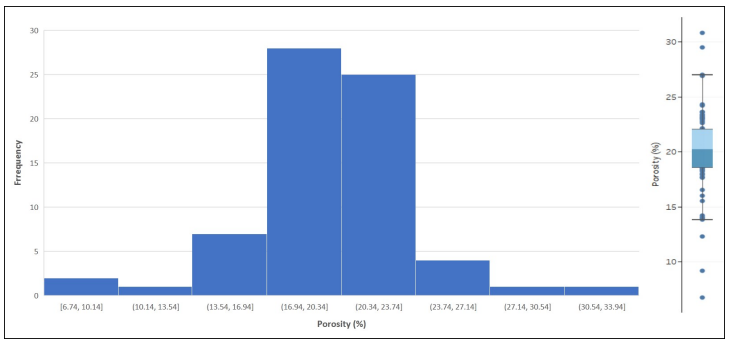

Figure 4.2. Porosity distribution on the incremental secondary recovery.

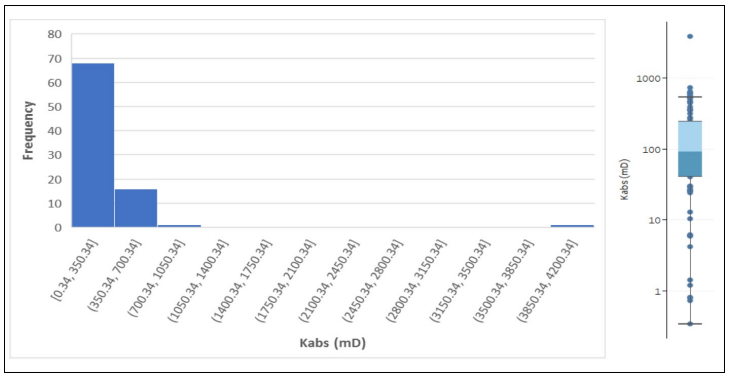

Figure 4.3. Permeability distribution on the incremental secondary recovery.

4.1.2. Tertiary Mode. In case of tertiary LSWF mode, Figure 4.4 shows the porosity-permeability relationship to the additional tertiary recovery. Most of the data indicate the additional tertiary recovery between 2 to 8% OOIP, despite the porosity and permeability values. The highest additional tertiary recovery (pointed by black arrow) is 19.4% OOIP from a consolidated sand rich in kaolinite and chert core in LC, Australia, with porosity of 26.9% and K_{abs} of 655 mD, which also produced high secondary recovery.

The other core that has high additional tertiary recovery of 18.2% (pointed by green arrow) is a core from Saudi reservoir with kaolinite mineral dominated. This core has porosity of 22.42% and K_{abs} of 78 mD. The recovery mechanism for this sandstone is

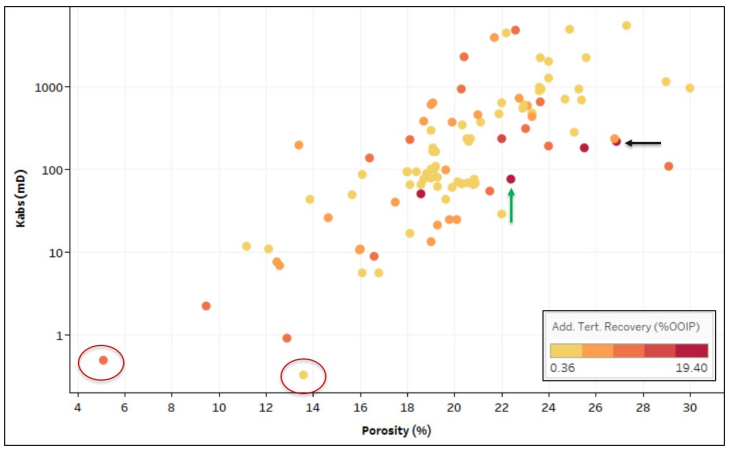

Figure 4.4. Porosity-permeability relationship to the additional tertiary recovery.

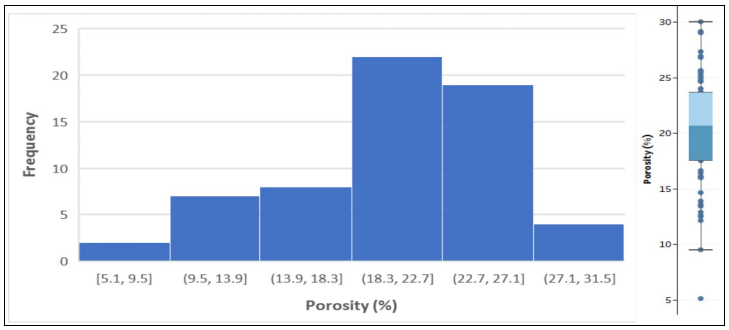

Figure 4.5. Porosity distribution on the additional tertiary recovery.

believed to refer to fines migration and the detachment of mixed-wet kaolinite clay particles (AlQuraishi *et al.*, 2015). The lowest porosity and the lowest permeability cores (circled in red) still produce the additional tertiary recovery of 8% and 3.4% OOIP, respectively.

The detail distribution of porosity and permeability that produce the additional tertiary recovery are depicted in Figures 4.5 and 4.6, respectively. The majority of data points fall in the porosity of 18-24% and the permeability of 51-653 mD.

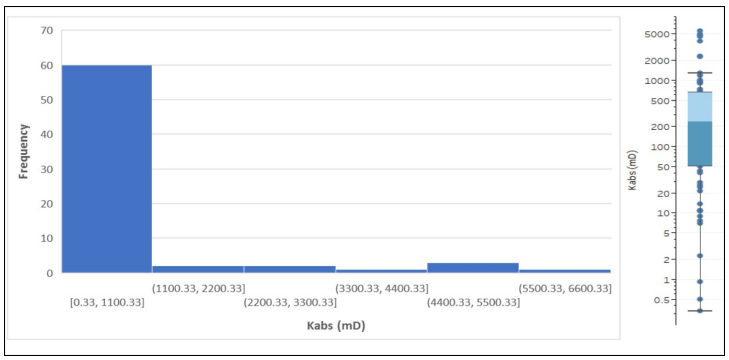

Figure 4.6. Pormeability distribution on the additional tertiary recovery.

4.2. EFFECT OF TOTAL CLAY CONTENT ON OIL RECOVERY

Based on the proposed LSWF mechanism, the clay minerals presence in the rock is one of the necessary conditions for low-salinity waterflooding (Bernard (1967); Lager *et al.* (2008a)). High CEC clay minerals are also favorable and their order should be: kaolinite < illite/mica < montmorillonite (Austad *et al.*, 2010).

4.2.1. Secondary Mode. Figure 4.7 shows the relationship between total clay content with incremental secondary recovery. Due to the importance of clay mineral types and data availability, the data points are displayed in term of kaolinite and illite/mica contents. The secondary mode crossplot indicates that the high recovery values are achieved by the cores with total clay content between 13 and 14 wt% (in green rectangle). The highest incremental recovery of 22% OOIP comes from a Berea core with total clay content of 14 wt%, kaolinite content of 5 wt% and illite/mica content of 1 wt%. A core with higher total clay content of 26 wt% gives incremental recovery of 9.24% OOIP (pointed by black arrow). This core is from Bandera sandstone with kaolinite content of 3 wt% and illite/mica content of 12 wt%. Nevertheless, there is a Berea core (in blue rectangle) with a high total clay content that produce very little incremental recovery, which conflicts with clay hydration and MIE mechanisms. The cores have total clay content of 17 wt%, with kaolinite and illite/mica content of 6.88 and 10.55 wt%, respectively. The permeability of these cores

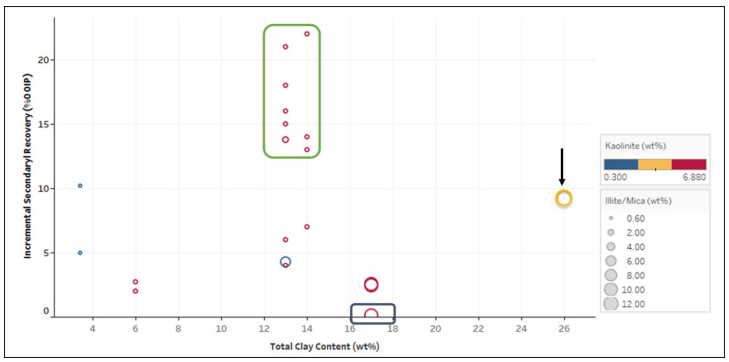

Figure 4.7. The relationship between total clay content and incremental secondary recovery.

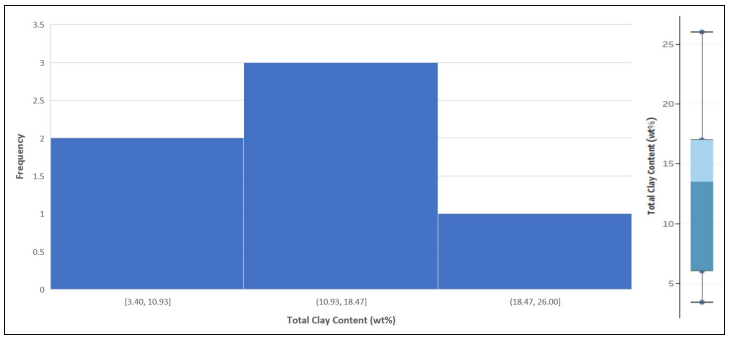

Figure 4.8. Total clay content distribution on the incremental secondary recovery.

is 6 mD. Kumar *et al.* (2016) concluded that high clay environments in low permeability sandstones and heavy oil reservoirs are not great targets for low-salinity waterflooding. It is because of possible plugging of pores upon fines migration and viscosity override of low-salinity water over crude oil. The total clay content distribution for this secondary mode is depicted in Figure 4.8.

4.2.2. Tertiary Mode. In the case of tertiary mode, there are not many data available as shown in Figure 4.9. However, it can be observed that the highest additional tertiary recovery of 13.6% OOIP (pointed by black arrow) comes from a North African Brown Sand core with high total clay content of 23 wt% and kaolinite and illite/mica content of 3.55 and 0.23 wt%, respectively. The data points in a black rectangle shows that no additional tertiary recovery are observed in the cores with total clay content of 13 wt% with kaolinite

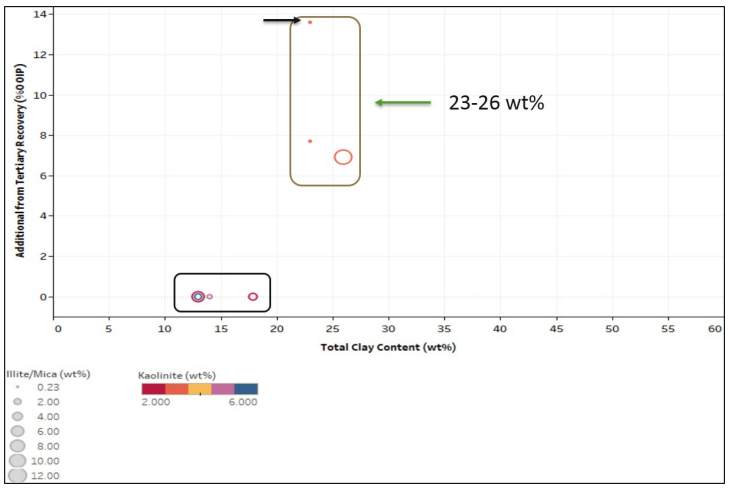

Figure 4.9. The relationship between total clay content and additional tertiary recovery.

and illite/mica content of 2 and 6 wt%, respectively. A core with 14 wt% total clay content also produces no additional recovery, which also conflicts with clay hydration and MIE mechanisms. This core has kaolinite content of 5 wt% and illite/mica content of 1 wt%. The cores that produced additional tertiary recovery have total clay content of between 23 and 26 wt%.

4.3. EFFECT OF CORE AGING TEMPERATURE & TIME ON OIL RECOVERY

Many researches found that high aging temperature drives a COBR system towards more oil wet and cause a high adsorption of oil components onto mica surfaces, that are beneficial for low-salinity waterflooding. The relationship between aging temperature and oil recovery in secondary and tertiary mode are plotted, with the data points are colored by aging time. Most of the corefloodings used the cores that aged ranging from 60 to 87 °C for both the secondary and tertiary mode.

4.3.1. Secondary Mode. There is no data trend in the secondary LSWF mode that is shown in Figure 4.10. The highest incremental recovery of 29.2% OOIP (pointed by black arrow) is achieved by a core that was aged in 75 °C for 10 days. It can be observed that if the

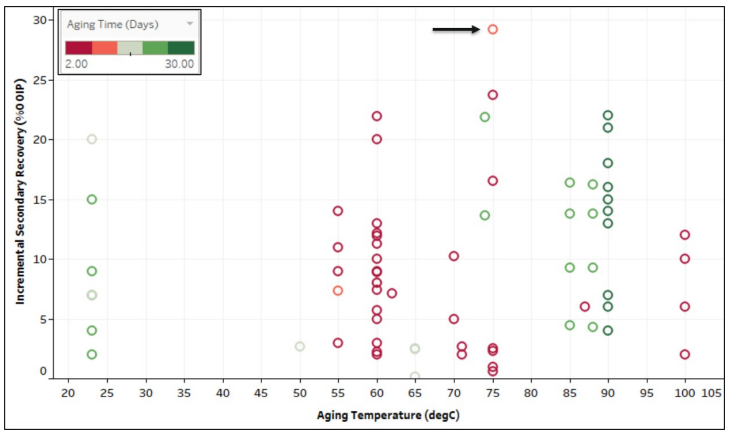

Figure 4.10. The relationship between aging temperature and incremental secondary recovery.

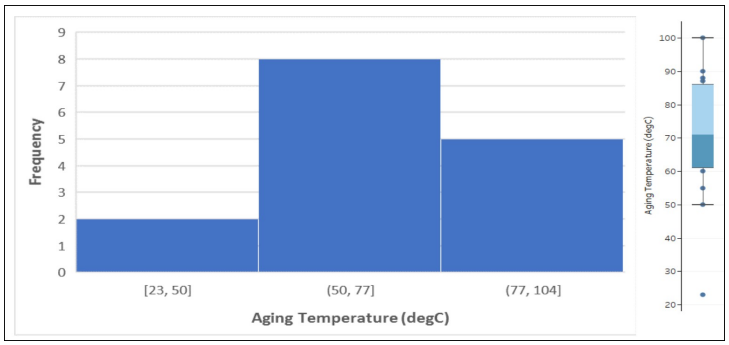

Figure 4.11. Aging temperature distribution on the incremental secondary recovery.

statement from Jadhunandan and Morrow (1995) was correct that higher aging temperature drives COBR towards oil-wet, this evidence conflicts with the mineral dissolution and water micro-dispersions mechanisms. The distribution of aging temperature of the cores that produced the incremental secondary recovery is depicted in Figure 4.11.

4.3.2. Tertiary Mode. The relationship between aging temperature and additional tertiary recovery is shown in Figure 4.12. The highest recovery is from a core that was also aged in 75 °C for 10 days (circled in green). The cores with low aging temperature of 40 °C for 7 days could produce high additional recovery up to 15.7% OOIP (circled in black). Different than the secondary mode, no additional tertiary recovery is observed

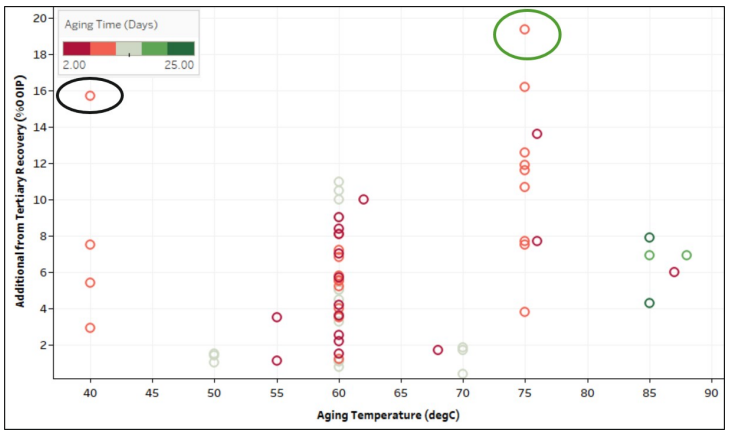

Figure 4.12. The relationship between aging temperature and additional tertiary recovery.

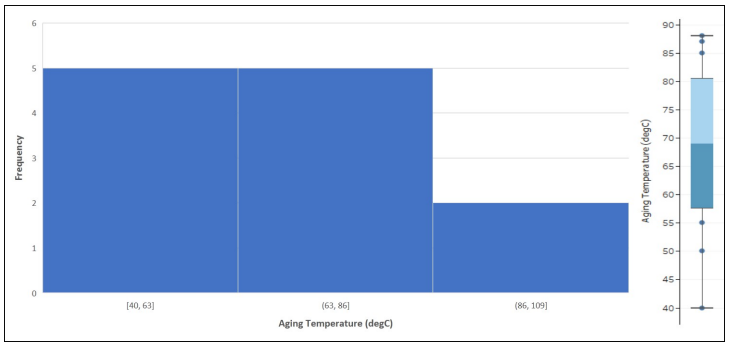

Figure 4.13. Aging temperature distribution on the additional tertiary recovery.

in the cores that were aged in higher temperature higher than 88 °C. The distribution of aging temperature of the cores that produced the additional tertiary recovery is depicted in Figure 4.13.

4.4. EFFECT OF CRUDE OIL/BRINE/ROCK WETTABILITY ON OIL RECOVERY

The wettability alteration is agreed as the dominant mechanism during LSWF by most of the researchers. Thus, there are many studies that performed to observe the effect of a crude oil/brine/rock (COBR) wettability to the improved oil recovery in the LSWF.

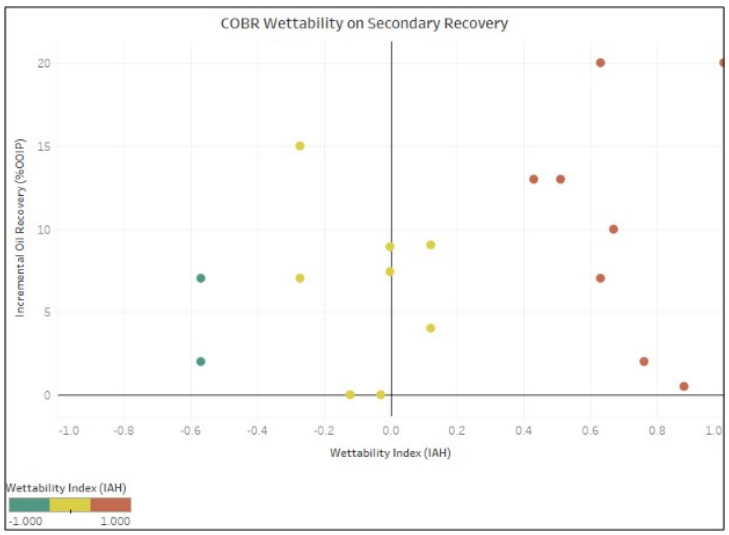

Figure 4.14. The relationship between COBR wettability and the incremental secondary recovery.

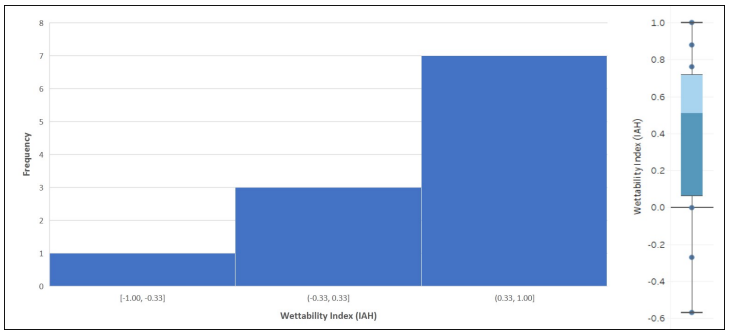

Figure 4.15. COBR wettability index distribution on the incremental secondary recovery.

4.4.1. Secondary Mode. Figure 4.14 shows the wettability index vs. incremental recovery in secondary LSWF mode. There is no exact trend found in this relationship, however, it is observed that high incremental recovery is achieved by water-wet ($0.3 \leq IAH \leq 1.0$) and intermediate-wet ($-0.3 \leq IAH \leq 0.3$) cores. This evidence supports the mineral dissolution and water micro-dispersions mechanisms. The distribution of wettability index that give the incremental secondary recovery is shown in Figure 4.15.

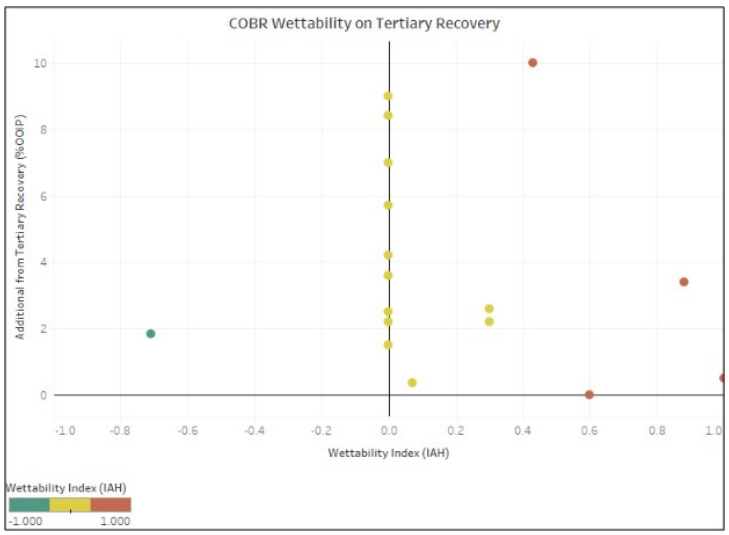

Figure 4.16. The relationship between COBR wettability and the additional tertiary recovery.

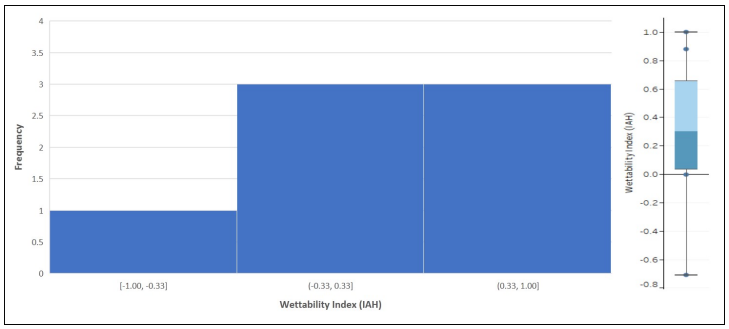

Figure 4.17. COBR wettability index distribution on the additional tertiary recovery.

4.4.2. Tertiary Mode. In the tertiary LSWF mode, which is shown in Figure 4.16, most of the data are intermediate-wet systems. The water-wet COBR system still gives the highest additional tertiary recovery, which is 10% OOIP. The intermediate-wet COBR system produces additional recovery between 0.36 to 9% OOIP. The distribution of wettability index that produce the additional tertiary recovery is shown in Figure 4.17.

4.5. EFFECT OF INITIAL WATER SATURATION ON OIL RECOVERY

In the LSWF process, the presence of initial water saturation is an important thing, as the increased in initial water saturation can decrease the adsorption of oil components on rock surfaces (Lager *et al.*, 2008a).

4.5.1. Secondary Mode. The relationship between initial water saturation and the incremental secondary recovery is shown in Figure 4.18. There is no trend can be observed in the secondary mode plot. However, there are three data points which show the high incremental recovery. The highest incremental recovery (circled in red), which is 42% OOIP, comes from Berea sandstone. This core has initial water saturation of 37.81%. It is followed by a core from LC, Australia, that produces incremental oil recovery of 29.2% OOIP with low initial water saturation of 13.2% (circled in green). These Berea and LC cores are also observed having high incremental recovery in the porosity-permeability plot. Another data point is a Berea core that has initial water saturation of 42.79%, and produces incremental recovery of 28% OOIP (circled in blue). The high incremental recovery in this core may be correlated with the acid and base functionalities in the oil that have a strong effect on wettability (Miyauchi *et al.*, 2017). This evidence supports MIE and pH-induced mechanisms. The lowest incremental secondary recovery of 0.13% OOIP was produced from a Berea core with a high initial water saturation of 41% (circled in orange). This core was flooded with monovalent KCL solution to test whether with K^+ being higher than Na^+ in the chemical reactivity series had any effect in replacement of the divalent cations during the potential MIE mechanism (Kumar *et al.*, 2016). The result shows that the low recovery could be because the formation clay may not have ready to accept K^+ as it did with Na^+.

Most of initial water saturation from the cores that produced the incremental secondary recovery are between 24 and 35%. The detail distribution of initial water saturation is depicted in Figure 4.19.

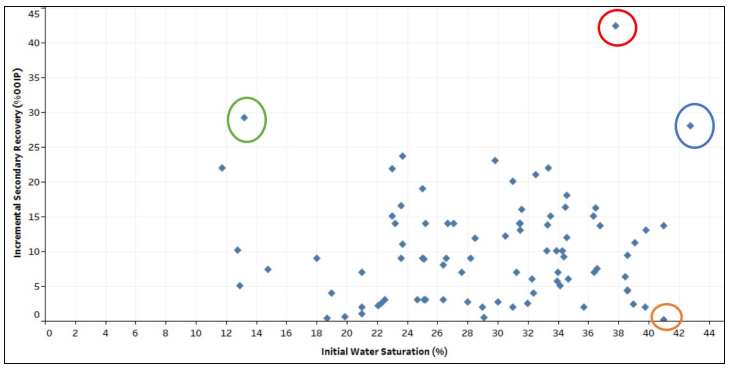

Figure 4.18. The relationship between initial water saturation and incremental secondary recovery.

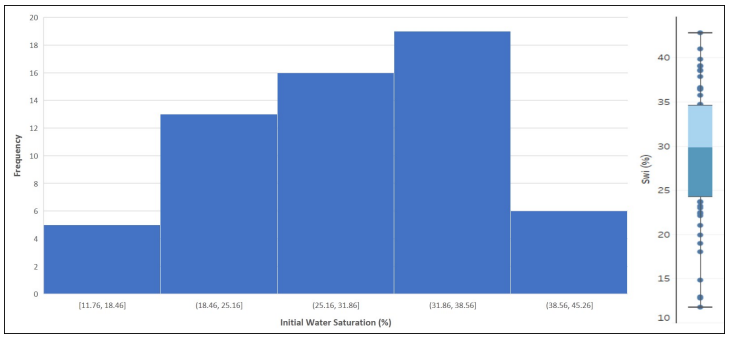

Figure 4.19. Initial water saturation distribution on the incremental secondary recovery.

4.5.2. Tertiary Mode. Figure 4.20 shows the relationship between initial water saturation and the additional tertiary recovery. There are also three data points that could be observed in the tertiary mode plot. The highest additional tertiary recovery of 19.4% OOIP is achived by a core from LC, Australia, that has initial water saturation of 13.6% OOIP (circled in red). It is followed by the core that has higher initial water saturation of 34.7% and produces additional tertiary recovery of 18.2% OOIP (circled in green). This core is from Saudi sandstone which is also observed in porosity-permeability plot. The other data point is a core with initial water saturation of 40.6% and produces additional recovery of 16.2% OOIP from LC, Australia, as well (circled in blue). However, this core contains formation brine that much more saline than the first LC core. The formation brine

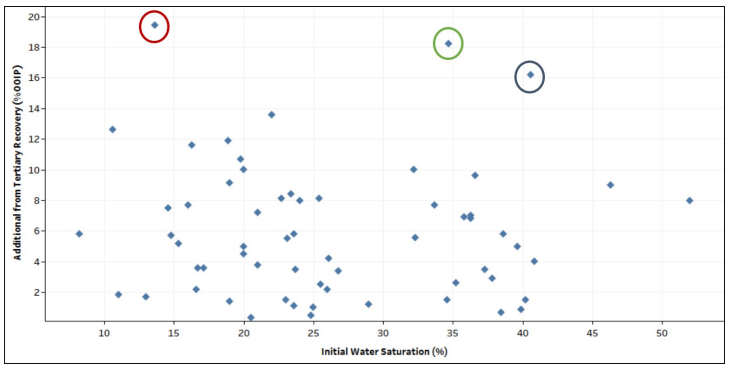

Figure 4.20. The relationship between initial water saturation and additional tertiary recovery.

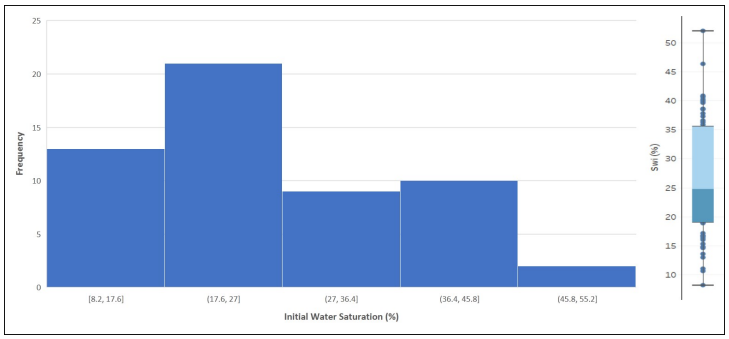

Figure 4.21. Initial water saturation distribution on the additional tertiary recovery.

salinity of this core is 29,690 ppm, while the first LC core has formation brine salinity of 1,480 ppm. The distribution of the initial water saturation from the cores that produced additional tertiary recovery is shown in Figure 4.21. From both secondary and tertiary modes, the distributions of initial water saturation show that the presence of connate water is important, which supports the EDL and MIE mechanisms.

4.6. EFFECT OF CRUDE-OIL BASE/ACID RATIO ON OIL RECOVERY

The low-salinity waterflooding process is also affected by the influence of crude oil. The polar components is believed must be present, and the acid and base number of the oil give a good quantitative indication of the active polar components. Some researchers

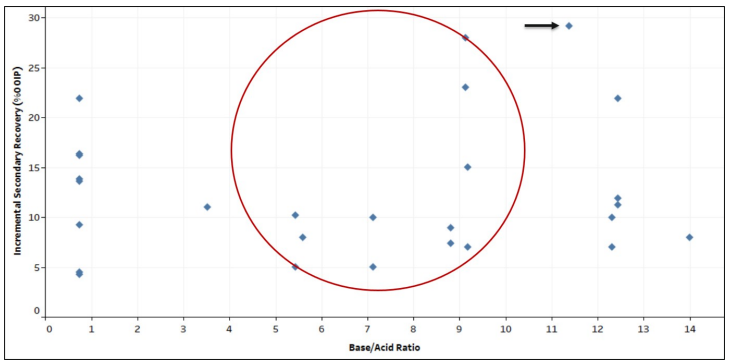

Figure 4.22. The relationship between crude oil base/acid ratio and incremental secondary recovery.

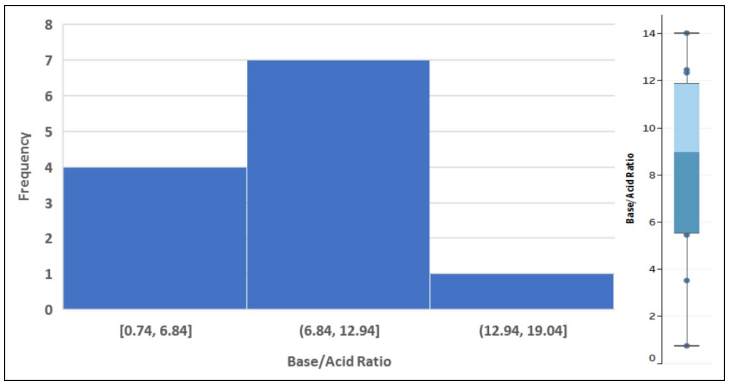

Figure 4.23. Crude oil base/acid ratio distribution on the incremental secondary recovery.

stated that the higher base/acid ratio, the higher retention of polar oil components. For the crude oil with high acidic components (low base/acid ratio), lower salinity gives higher retention of polar oil components. While, for the crude oil with low acidic components (high base/acid ratio), the retention of polar oil components was found not to be much affected by the brine composition.

4.6.1. Secondary Mode. Figure 4.22 depicts the relationship between crude oil base/acid ratio and the recovery in secondary LSWF mode. The highest recovery of 29.2% OOIP (pointed by black arrow) comes from the crude oil with base/acid ratio of 11.38 (low acidity). The majority of the corefloodings used crude oil with base/acid ratio of between 6 and 12, as also shown in Figure 4.23.

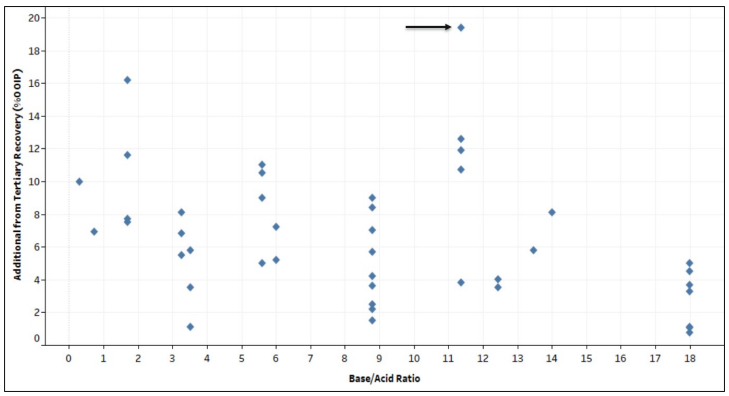

Figure 4.24. The relationship between crude oil base/acid ratio and additional tertiary recovery.

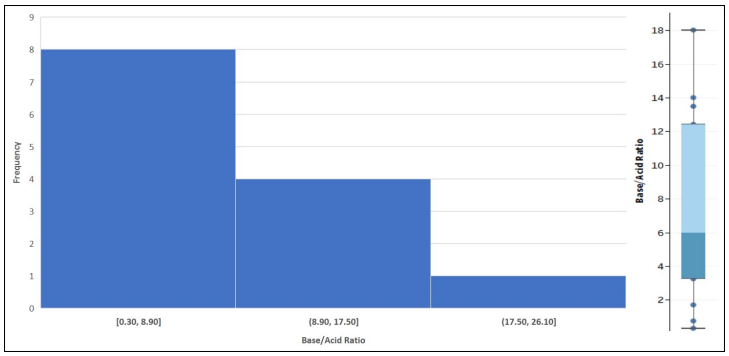

Figure 4.25. Crude oil base/acid ratio distribution on the additional tertiary recovery.

4.6.2. Tertiary Mode. Figure 4.24 shows the the relationship between crude oil base/acid ratio and the additional tertiary recovery. The high additional tertiary recoveries come from the oil with high acidity components (low base/acid ratio). The low base/acid ratio of 1.71 could produce additional tertiary recovery up to 16.2% OOIP. However, the highest additional tertiary recovery of 19.4% OOIP (pointed by black arrow) comes from the crude oil with base/acid ratio of 11.38 (low acidity), same as the case in secondary mode. Most of the data points range from 0.3 to 9, as shown in Figure 4.25.

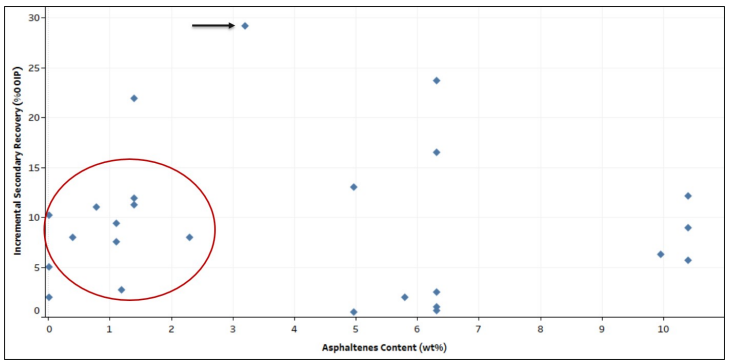

Figure 4.26. The relationship between crude oil asphaltenes content and incremental secondary recovery.

4.7. EFFECT OF ASPHALTENES CONTENT ON OIL RECOVERY

The asphaltenes content in the crude oil is also one parameter which affects the retention of polar oil components. Crocker and Marchin (1988) stated that the crude oil with high composition of asphaltenes and resins will retain more on reservoir rocks through direct adsorption and drive the COBR system towards a more oil-wet system.

4.7.1. Secondary Mode. The relationship between asphaltenes content in the crude oil and the incremental secondary recovery is shown in the Figure 4.26. The highest incremental recovery is achieved by the oil with 3.2 wt% asphaltenes content (pointed by black arrow). The lower asphaltenes content of between 0 and 1.4 wt% could produce oil recovery up to 21.92% OOIP (circled in red). Whereas, the higher asphaltenes content of 10.4 wt% could give incremental recovery up to 12.14% OOIP. The distribution of asphaltenes content in the crude oil that can produce the incremental secondary recovery is shown in Figure 4.27.

4.7.2. Tertiary Mode. In the case of tertiary mode, Figure 4.28 shows that the crude oil with the lowest asphaltenes content of 0.4 wt% could give 8.1% OOIP additional recovery (pointed by black arrow), while the oil with highest asphaltenes content of 10.4 wt% produced lower than the one with the lowest asphaltenes content, which is 5.6% OOIP

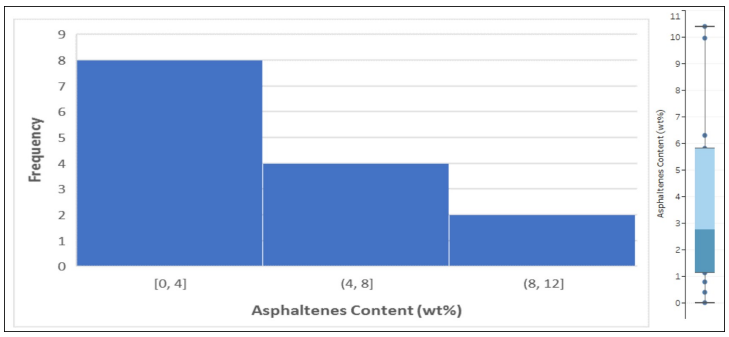

Figure 4.27. Crude oil asphaltenes content distribution on the incremental secondary recovery.

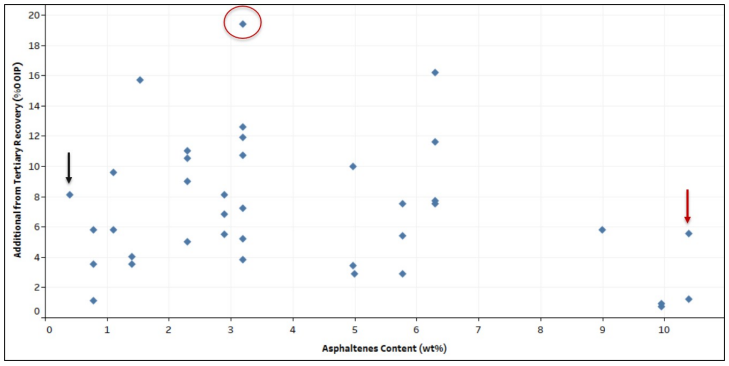

Figure 4.28. The relationship between crude oil asphaltenes content and additional tertiary recovery.

additional tertiary recovery (pointed by red arrow). The majority of asphaltenes content are between 0.4 and 6 wt% as depicted in Figure 4.29. From both secondary and tertiary mode plots, it can be observed that asphaltenes content in the crude oil is not necessary, which conflicts to the MIE and pH-induced mechanisms.

4.8. EFFECT OF FORMATION BRINE SALINITY & DIVALENT CATIONS ON OIL RECOVERY

The experiments conducted by Shehata and Nasr-El-Din (2015) shows that reservoir cores saturated with connate water containing divalent cations of Ca^{2+} and Mg^{2+} showed higher oil recovery than for cores saturated with monovalent cation Na^{+}. The divalent

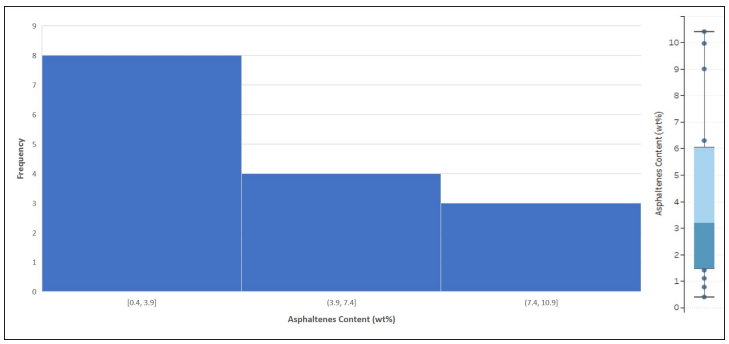

Figure 4.29. Crude oil asphaltenes content on the additional tertiary recovery.

cations concentration in the formation brine is presented as a percentage of formation brine $CaCl_2$ and $MgCl_2$ concentrations. It is calculated as follows:

$$\%\, of\ Form.\ Brine\ Divalent\ Ions\ = \frac{Form.\ Brine\ Divalent\ Ions\ Salinity\ (ppm)}{Formation\ Brine\ Salinity\ (ppm)} x100\%. \tag{4.2}$$

4.8.1. Secondary Mode. The relationship between divalent ions concentration in the formation brine and oil recovery in secondary mode is depicted in Figure 4.30. It can be observed that the low divalent ions concentration in the formation brine could produce a high incremental secondary recovery (circled in red). The highest incremental secondary recovery of 42.4% OOIP was produced from the core that does not have divalent ions (Ca^{2+} and Mg^{2+}). It is followed by the incremental secondary recovery of 29.2% OOIP that was produced from a core that has 3.4% of divalent ions concentration in the formation brine. This coreflooding used the formation brine salinity of 29,690 ppm. On the other side, the high divalent ions concentration in the formation brine produced a low incremental secondary recovery (circled in green), conflicting with the EDL and MIE mechanisms. The divalent ions concentration of 30.6% in the formation brine could only produce the incremental secondary recovery up to 2.43% OOIP. This low recovery might be because

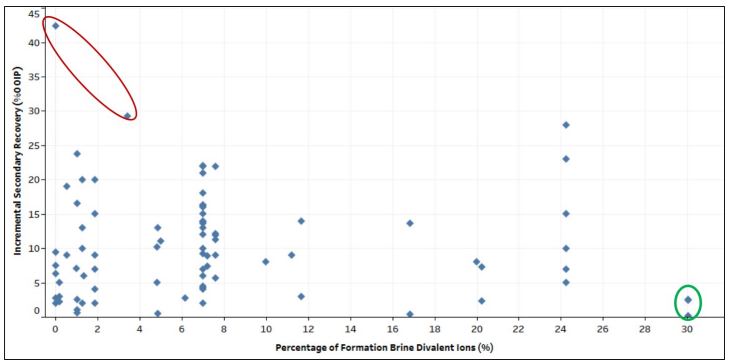

Figure 4.30. The relationship between formation brine divalent ions concentration and incremental secondary recovery.

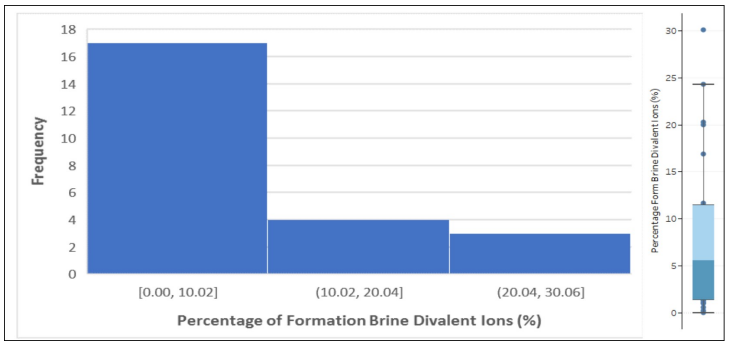

Figure 4.31. Formation brine divalent ions concentration on the incremental secondary recovery.

there was only a little of fines migration observed when the core was flooded by $MgCl_2$ solution (Kumar *et al.*, 2016). The distribution of the percentage of formation brine divalent ion concentration on the secondary mode is shown in Figure 4.31.

4.8.2. Tertiary Mode. Figure 4.32 shows similar to the secondary mode plot that the low divalent ions concentration in the formation brine could produce a high additional tertiary recovery (circled in red). The 0% of divalent ions concentration in the formation brine could give the additional tertiary recovery of 13.6% OOIP, and 3.41% of divalent ions concentration could produce the additional recovery of 16.2% OOIP. The distribution of of the percentage of formation brine divalent ion concentration on the tertiary mode is depicted in Figure 4.33.

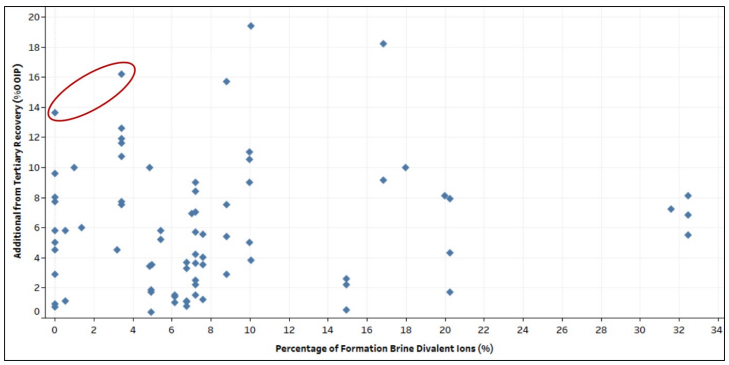

Figure 4.32. The relationship between formation brine divalent ions concentration and additional tertiary recovery.

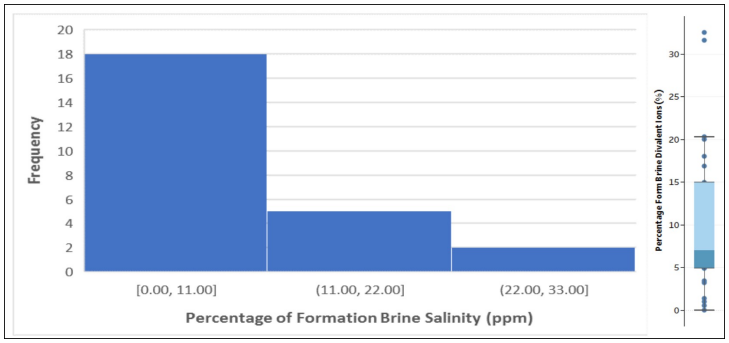

Figure 4.33. Formation brine divalent ions concentration on the additional tertiary recovery.

4.9. EFFECT OF INJECTED BRINE SALINITY & DIVALENT ION CONCENTRATION ON OIL RECOVERY

Nasralla and Nasr-El-Din (2011) concluded that as long as the injected brine was $CaCl_2$ free, decreasing the concentration of NaCl in injected brine did not affect the amount of Ca^{2+} exchange between the brine and the rock.

4.9.1. Secondary Mode. Figure 4.34 shows the correlation between injected brine salinity with the incremental secondary recovery. The data points are displayed in term of $CaCl_2$ and NaCl concentrations. The data points circled in red show high incremental recoveries that come from the injected brine salinity with low $CaCl_2$ concentration. The highest incremental recovery (pointed by black arrow) is achieved by the core flooded by

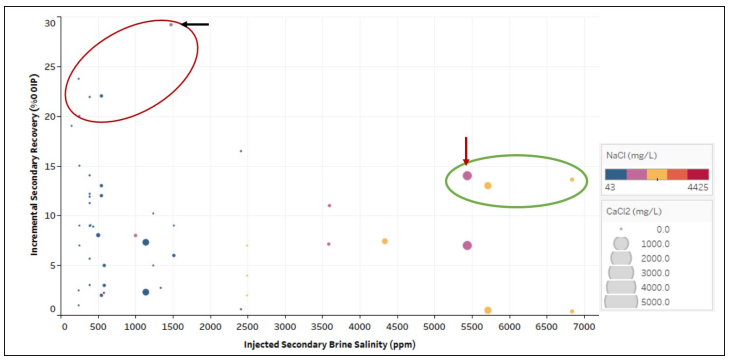

Figure 4.34. The relationship between injected brine salinity and incremental secondary recovery.

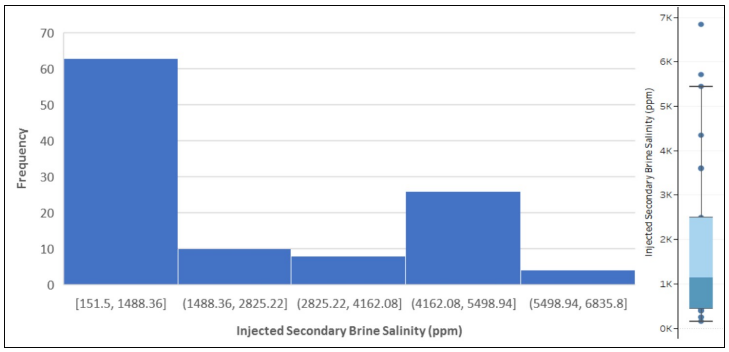

Figure 4.35. Injected brine salinity distribution on the incremental secondary recovery.

brine salinity of 1,480 ppm, with $CaCl_2$ concentration of 47.1 mg/L and NaCl concentration of 1,135 mg/L. However, there are also some data points (circled in green) that show high incremental recoveries from the injected brine salinity with higher $CaCl_2$ concentration. For instance, there is a data point (pointed by red arrow) that shows high incremental recovery from the injected brine salinity of 5,436 ppm, with $CaCl_2$ concentration of 392 mg/L and NaCl concentration of 1,504 mg/L. Thus, it indicates that $CaCl_2$ free in the injected secondary brine is not necessary. Majority of the corefloodings used the injected brine with salinity of between 151.5 and 1488 ppm, as shown in Figure 4.35.

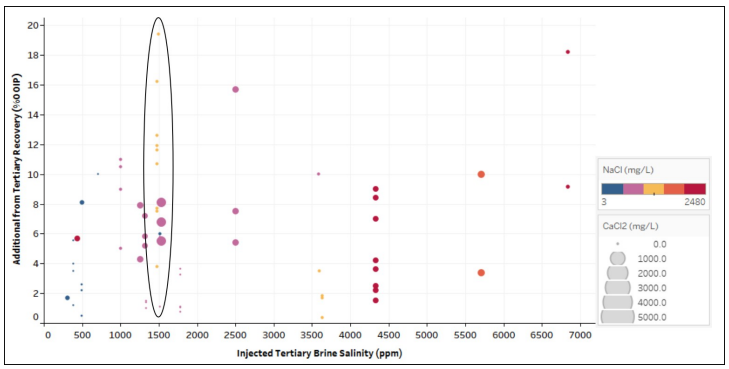

Figure 4.36. The relationship between injected brine salinity and additional tertiary recovery.

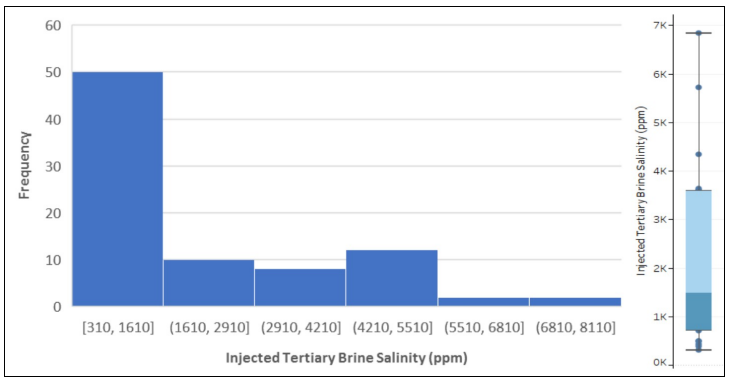

Figure 4.37. Injected brine salinity distribution on the additional tertiary recovery.

4.9.2. Tertiary Mode. Figure 4.36 indicates there are data points (circled in black) that show low injected tertiary brine salinity of 1,480 ppm, with $CaCl_2$ concentration of 47.1 mg/L and NaCl concentration of 1,135 mg/L which produced the high additional tertiary recovery up to 19.4% OOIP. From both secondary and tertiary mode plots, it can be observed that even though $CaCl_2$ free in the injected brine is not necessary, the high recovery values are gained from the low concentration of $CaCl_2$. The distribution of injected tertiary brine salinity on the additional tertiary recovery is shown in Figure 4.37.

4.10. EFFECT OF FORMATION & INJECTED BRINE SALINITY RELATIONSHIP ON OIL RECOVERY

Tang and Morrow (1999) concluded that in the case of identical formation brine injected brine salinity, final oil recovery increased when the injection brine salinity was lowered. The researchers also discovered that the injected brine salinity was sensitive to formation brine salinity, however the difference in final recovery was much smaller.

Figure 4.38 and 4.39 are displayed in order to observe the relationship between formation brine salinity and how much the injected brine salinity were reduced or diluted to gain the highest incremental secondary recovery and additional tertiary recovery during the low-salinity waterflooding. The conventional waterflooding salinity vs. formation brine salinity plot is also displayed to give information on the high-salinity brine that is injected to a rock with certain formation brine salinity value. For instance, in the secondary LSWF stage, the highest incremental secondary recovery that could be produced from a rock that has 100,000 ppm formation brine salinity, is 8% OOIP, when it is injected by the low-salinity brine that has been diluted 200 times, compared to 40,000 ppm high-salinity brine injection. As well as in the tertiary LSWF stage, for instance, a rock that has formation brine salinity of 100,000 ppm, could produce the highest additional tertiary of recovery of 10% OOIP, when it is injected by the low-salinity brine that has been diluted 35 times, after the injection of 25,000 ppm high-salinity brine in the conventional waterflooding.

4.11. EFFECT OF LSWF RECOVERY STAGE ON FINAL OIL RECOVERY

One of the objectives of this study is to observe in what EOR stage/mode the low-salinity waterflooding is best implemented. Figure 4.40 shows the boxplots of final recovery in secondary, tertiary, and secondary+tertiary LSWF stages, and also to compare the LSWF to the conventional (high-salinity) waterflooding. The boxplots are labeled by the minimum and maximum values in each stage.

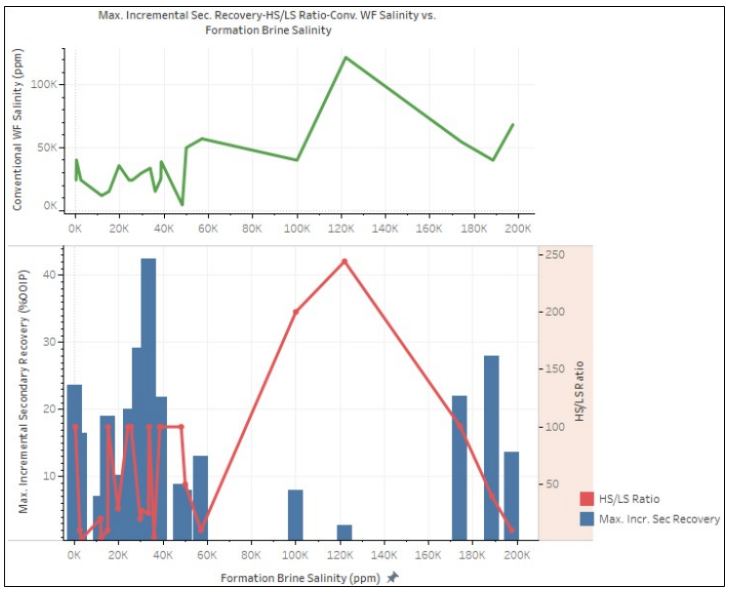

Figure 4.38. Maximum incremental secondary recovery-formation brine-HS/LS ratio relationship and conventional WF salinity.

The final recovery in secondary+tertiary LSWF mode reaches the highest maximum value of 86.66% OOIP, followed by the secondary LSWF with the maximum value of 86% OOIP, whereas the lowest maximum value for the LSWF is in the tertiary stage. The highest minimum values of the LSWF stages is also gained by the secondary+tertiary mode. The lowest value of minimum final recovery is 15.4% OOIP in the tertiary LSWF mode. It comes from the Berea core that was flooded with 250,000 ppm brine and produced 10% OOIP recovery at the secondary stage. By injecting 2,500 ppm brine into the core, the additional 5.4% OOIP of recovery was observed (Ishiwata *et al.*, 2016). In comparison to the conventional waterflooding, the final recovery from all of the LSWF stages are higher than the one of conventional waterflooding. It can be observed that based on the data collection, the EOR low salinity-waterflooding is more beneficial than the conventional waterflooding, in term of the final recovery produced.

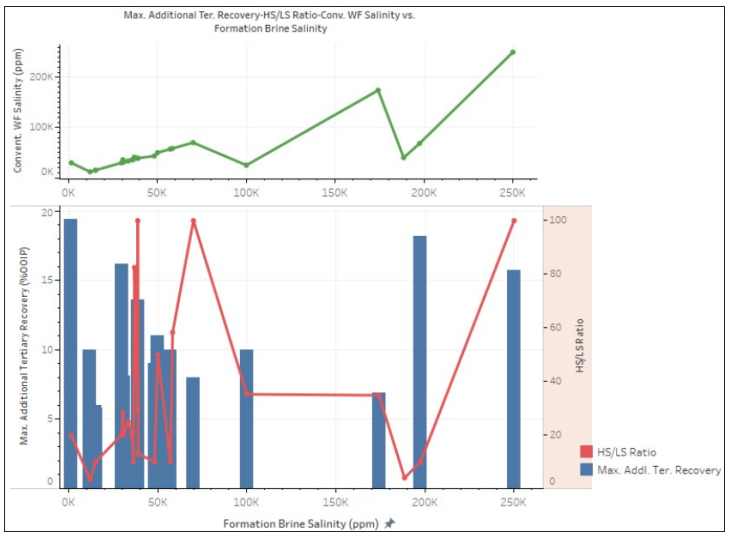

Figure 4.39. Maximum additional tertiary recovery-formation brine-HS/LS ratio relationship and conventional WF salinity.

4.12. SUMMARY OF THE APPLICABILITY

The applicability of parameters affecting the low-salinity waterflooding process in secondary and tertiary modes are summarized in Tables 4.1 and 4.2. It is necessary to be noted that this applicability is based on the coreflooding experiments in this study.

Table 4.1. Applicability of parameters impacting LSWF in secondary mode.

Parameter	Minimum	Maximum	Median	Mean
Porosity (%)	6.7	30.8	20	20.2%
Permeability (mD)	0.3	3,900	215	93%
Wettability Index (IAH)	-0.57	1	0.38	0.51%
Initial Water Saturation (%)	11.8	42.8	29.3	29.8%
Total Clay Content (wt%)	3.4	26	13.2	13.5%
Aging Temperature (°C)	23	100	70.3	71%
Base/Acid Ratio	0.74	14	8.3	9%
Asphaltenes Content (wt%)	0	10.4	3.8	2.8%
Formation Brine Salinity (ppm)	242	197,451	51,652	33,545%
% of Form. Brine Divalent Ions	0	30	8.2	5.6%
Injected Brine Salinity (ppm)	152	6,836	1,862	1,140%
HS/LS Ratio	3.3	244	53.1	27.8

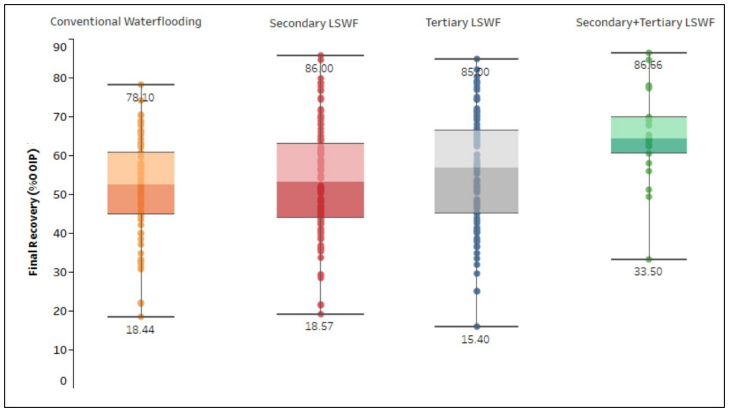

Figure 4.40. Boxplots of final recovery in each LSWF stage and conventional waterflooding.

Table 4.2. Applicability of parameters impacting LSWF in tertiary mode.

Parameter	Minimum	Maximum	Median	Mean
Porosity (%)	5.1	30	20.4	20.7%
Permeability (mD)	0.3	5,570	712	238%
Wettability Index (IAH)	-0.71	1	0.28	0.3%
Initial Water Saturation (%)	8.2	52	26.5	24.8%
Total Clay Content (wt%)	23	26	24.5	24.5%
Aging Temperature (°C)	40	88	68	69%
Base/Acid Ratio	0.3	18	7.6	6%
Asphaltenes Content (wt%)	0.4	10.4	4.3	3.2%
Formation Brine Salinity (ppm)	1,480	250,000	57,114	36,318%
% of Form. Brine Divalent Ions	1	32.5	9.9	7%
Injected Brine Salinity (ppm)	310	6,836	2,080	1,490%
HS/LS Ratio	3.3	312.1	51	24.3

5. CONCLUSIONS AND RECOMMENDATIONS

Studies performed in this thesis are data analyses from many laboratory experiments and field cases found in the literature. The studies revealed the complexity of LSWF mechanisms and the corresponding parameters in the crude/oil/brine/rock system that associate with this process. The present section summarizes the conclusions stemming from the studies and provides recommendations for future work.

5.1. CONCLUSIONS

This work collects data from various published literature to develop a comprehensive data set regarding low-salinity waterflooding to enhance oil recovery in sandstone reservoirs. The LSWF mechanisms are discussed in the literature review section to gain better understanding of the LSWF effect on oil recovery in sandstone reservoirs. The data set consists of parameters from laboratory coreflooding experiments that involved core samples, crude oil, and brines from different places. Histograms and boxplot are used to visualize various kinds of data and their ranges. The cross plots and bar charts are used to analyze the relationship between the important parameters and oil recovery. The important parameters, such as rock porosity and permeability, total clay content, core aging temperature, COBR wettability, initial water saturation, oil base/acid ratio, asphaltenes content, formation and injected brine salinity and composition are analyzed in the case of secondary and tertiary low-salinity waterflooding modes. The following conclusions are drawn from the studies:

1. There are ten proposed LSWF mechanisms that discussed in this thesis, which most of these mechanisms are related to and/or conflicting each other. In addition, there are ten field cases data from ten references, which are discussed in the literature review section.

2. There are many important parameters involved in a COBR system that affect the enhanced oil recovery during LSWF process. They include the rock porosity and permeability, total clay content, core aging temperature, COBR wettability, initial water saturation, crude-oil base/acid ratio, asphaltenes content, formation and injected brine salinity, and brine composition.

3. The highest number of sandstone type that were used in the coreflooding experiments is Berea sandstone, which is 233 data. The Berea sandstone has relatively high porosity and permeability, thus those make it a good reservoir rock.

4. In the relationship of both porosity and permeability to the incremental oil recovery in the secondary LSWF mode, most of the data show the incremental oil recovery between 4 to 16% OOIP, regardless the porosity and permeability values. The highest incremental recovery is 42% OOIP from the Berea core that has porosity and K_{abs} of 20.33% and 351.8 mD, respectively. In the tertiary LSWF mode, most of the data indicate the additional tertiary recovery between 2 to 8% OOIP, despite the porosity and permeability values. The highest additional tertiary recovery is 19.4% OOIP from a consolidated sand rich in kaolinite and chert core in LC, Australia, with porosity of 26.9% and K_{abs} of 655 mD, which also produced high secondary recovery.

5. There is no exact trend found in the relationship between wettability index vs. oil recovery, however, it is observed that high incremental and additional oil recovery are achieved by water-wet ($0.3 \leq IAH \leq 1.0$) and intermediate-wet ($-0.3 \leq IAH \leq 0.3$) cores.

6. The presence of connate water is important in both secondary and tertiary LSWF modes. Most of initial water saturation from the cores that produced the incremental secondary and additional tertiary recoveries range from 24 to 35% and from 19 to 36%, respectively.

7. Clay minerals must be present during LSWF process, but no kaolinite and illite/mica presence are necessary. The secondary mode crossplot indicates that the high recovery values are achieved by the cores with total clay content between 13 and 14 wt%. The cores that produced additional tertiary recovery have total clay content of between 23 and 26 wt%. Nevertheless, no additional tertiary recovery are observed in the cores with total clay content of 13 wt% with kaolinite and illite/mica content of 2 and 6 wt%, respectively. A core with 14 wt% total clay content also produces no additional recovery. This core has kaolinite content of 5 wt% and illite/mica content of 1 wt%.

8. The highest incremental secondary recovery of 29.2% OOIP is achieved by a core that was aged in 75 °C for 10 days. The cores with low aging temperature of 40 °C for 7 days could produce high additional tertiary recovery up to 15.7% OOIP.

9. In the secondary LSWF mode, the highest recovery of 29.2% OOIP comes from the crude oil with high base/acid ratio of 11.38 (low acidity). Whereas, in the tertiary LSWF mode, the higher additional tertiary recovery come from the oil with higher acidity components (low base/acid ratio).

10. The highest incremental secondary recovery is achieved by the oil with 3.2 wt% asphaltenes content. The lower asphaltenes content of between 0 and 1.4 wt% could produce oil recovery up to 21.92% OOIP. Whereas, the higher asphaltenes content of 10.4 wt% could give incremental recovery up to 12.14% OOIP. In the case of tertiary mode, the lowest asphaltenes content of 0.4 wt% could give 8.1% OOIP additional recovery, while the oil with highest asphaltenes content of 10.4 wt% produced lower than the one with the lowest asphaltenes content, which is 5.6% OOIP additional tertiary recovery.

11. The low divalent ions concentration in the formation brine could produce a high recovery in both secondary and tertiary LSWF mode.

12. From both secondary and tertiary mode plots, it can be concluded that even though $CaCl_2$ free in the injected brine is not necessary, the high recovery values are gained from the low concentration of $CaCl_2$.

13. It is observed the relationship between formation brine salinity and how much the injected brine salinity from normal waterflooding were reduced or diluted to gain the low-salinity injected brine that produced the highest incremental secondary recovery and additional tertiary recovery during the low-salinity waterflooding.

14. The applicability of parameters affecting the low-salinity waterflooding process in secondary and tertiary modes are summarized.

15. The final recovery in secondary-tertiary LSWF mode reaches the highest maximum value of 86.66% OOIP, followed by the secondary LSWF with the maximum value of 86% OOIP, whereas the lowest maximum value for the LSWF is in the tertiary stage. The highest minimum values of the LSWF stages is also gained by the secondary-tertiary mode. The lowest value of minimum final recovery is 15.4% OOIP in the tertiary LSWF mode.

16. In comparison to the conventional waterflooding, the final recovery from all of the LSWF stages are higher than the one of conventional waterflooding. Therefore, based on the data collection, the EOR low salinity-waterflooding is more beneficial than the conventional waterflooding, in term of the final recovery produced.

5.2. RECOMMENDATIONS FOR FUTURE WORK

The data analysis in this thesis uses some important parameters to observe the effect on the oil recovery. However, due to the data availability, the effect of pH on the oil recovery is not included. Further investigation is needed because a literature reported that different

clays have different adsorption/desorption window and the injection of low salinity brine will cause desorption of adsorbed cations, which will increase the pH close to the water-wet clay interface (Austad *et al.*, 2010).

The permeability reduction is also not investigated in this thesis. Further observation is necessary to see if the LSWF effects are accompanied by permeability reduction. In addition, it is needed to observe the variation in end-point relative permeability data between high- and low-salinity waterfloodings.

It is sometime hard to see the trend from the crossplots of some parameters. The clustering method is possible to use in the future work, in order to identify groups of similar corefloodings properties in this kind of multivariable data set. Any clustering techniques can be approached and will be beneficial because the LSWF mechanisms involve many different type of parameters, such as core, oil, and brine properties, as well as the COBR system itself. It is expected that the clustering method will help in obtaining clear trend and relationship between a parameter and oil recovery.

APPENDIX

SUMMARY OF PROPOSED LSWF MECHANISMS

Table A1. Summary of proposed LSWF mechanisms.

No	Mechanisms	Factors	References	Counterevidences
1	Clay Hydration (1967)	Clay contained in a rock; Clays hydrate and swell	SPE-1725-MS (1967); Illinois State Geo.Survey (1955)	Improved oil recovery by LSWF in clay-free core (SPE-172778/2017)
2	Fines Migration (1999)	Detachment of clay particles increase oil mobility; Kaolinite must be present	JPSE-24-99-111 (1999); SPE-176548-MS (2015)	BP LSWF coreflooding showed increase oil recovery with no fine migration (SPWLA-2008-v49n1a2); Improved recovery by kaolinite-free core (SPE-124277/2009)
3	Alkaline-Flooding Behavior (2005)	Generation of in-situ surfactant; Wettability alteration; Clay particles detachment	SPE-93903-MS (2005)	A pH increase is not reported in all experiments, and not as high as alkaline flooding (SPE-129767/2010)
4	Multicomponent Ionic Exchange-MIE (2006)	Ion exchanges between crude oil polar components and divalent cations	SPWLA-2008-v49n1a2 (2008); SPE-124277-MS (2009); SPWLA-2010-v51n5a2 (2010); SPE-149077-MS (2011); SPE-169090-MS (2014); SPE-170807-MS (2014); SPE-176492-MS (2015); SPWLA-JFES-2016-M	Presence of divalent cations in the injected brine is not critical (SPE-93903/2005); LSWF could be applied for light oil with more paraffinic content (SPE-189249/2017)
5	Salting-in Effect -A Chemical Mechanism (2009)	Solubility of organic polar compounds promote water-wettability of the rock	Energy Fuels 2009, 23, 4479-4485: DOI:10.1021/ef900185q	No correlation between desorption of hydrocarbon on kaolinite surface and injected brine condition (SPE-129767/2010)

Table A2. Summary of proposed LSWF mechanisms (continued).

No	Mechanisms	Factors	References	Counterevidences
6	Electric Double Layer-EDL (2009)	Water layer thickens as double layer expands, causes clay surface more water wet	SPE-119835-MS (2009); SPE-129722-MS (2010); SPE-129012-MS (2010); SPE-144602-MS (2011); SPE-154334-PA (2012); SPE-174063-MS (2015); SPE-180874-MS (2016)	Adsorption of divalent ions at the oil/water and water/rock interfaces changes the water-wet to oil-wet in the presence of Na^+ (JPSE-59-2007 p.147-156)
7	Mineral Dissolution (2010)	Dissolution of anhydrate creates an acidic pH, changes the rock from weak to stronger water-wet	JPSE-24-99-111 (1999); SPE-176548-MS (2015)	Based on this mechanism, the presence of clay is not necessary for LSWF process, which contradicts numerous studies
8	pH Induced Wettability Change-A Chemical Mechanism (2010)	Increase in pH because Ca^{2+} is substituted by H^+; Water wettability is improved; Extension of MIE and Salting-in	SPE-129767-MS (2010); SPE-169090-MS (2014); SPE-179625-MS (2016)	The pH value at the effluent end could increase or decrease depending on other chemical reactions (Austad, 2013)
9	Water Microdispersions (2013)	Water microdispersion form at oil/water interface, causes depletion of the interface; Wettability alteration	SPE-166435-MS (2013); SPE-172778-PA (2017); SPE-188512-MS (2017); SPE-183695-MS (2017)	No validity of this hypothesis by other researchers

Table A3. Summary of proposed LSWF mechanisms (continued).

No	Mechanisms	Factors	References	Counterevidences
10	Osmosis - A novel hypothesis (2016)	Osmosis occurs in COBR system because the system full of excellent semipermeable membrane (oil itself)	SPE-179741-PA (2016); SPE-180060-MS (2016); SPWLA-2017-v58n1a3	Coreflooding experiment using mineral oil (oil without polar components) did not show any additional oil recovery

REFERENCES

Abdulla, F., Hashem, H. S., Abdulraheem, B., Al-Nnaqi, M., Al-Qattan, A., John, H., Cunningham, P. R. P., Briggs, P. J., Thawer, R., and Manama, B., 'First eor trial using low salinity water injection in the greater burgan field, kuwait,' SPE-164341-MS, 2013, doi:10.2118/164341-MS.

Akhmetgareev, V. and Khisamov, R., 'Incremental oil recovery due to low-salinity waterflooding: Pervomaiskoye oil field case study (russian),' SPE-182043-RU, 2016, doi:10.2118/182043-RU.

Alden, A., https://www.thoughtco.com/all-about-sediment-grain-size-1441194, 2017, accessed: 02-04-2018.

AlQuraishi, A. A., AlHussinan, S. N., and AlYami, H. Q., 'Efficiency and recovery mechanisms of low salinity water flooding in sandstone and carbonate reservoirs,' OMC-2015-223, 2015, doi:0788894043648.

Alvarado, V., Garcia-Olvera, G., Hoyer, P., and Lehmann, T. E., 'Impact of polar components on crude oil-water interfacial film formation: A mechanisms for low-salinity waterflooding,' SPE-170807-MS, 2014, doi:10.2118/170807-MS.

Alvarez, C., http://gaffney-cline-focus.com/optimal-design-pilot-tests-english, 2017, accessed: 02-04-2018.

Amyx, J. W., Bass, D. M., and Whiting, R. L., *Petroleum Reservoir Engineering: Physical properties*, McGraw-Hill, 1960.

Anderson, W., 'Wettability literature survey- part 2: Wettability measurement,' SPE-13933-PA, 1986, doi:10.2118/13933-PA.

Ashraf, A., Hadia, N., Torsaeter, O., and Tweheyo, M. T., 'Laboratory investigation of low salinity waterflooding as secondary recovery process: Effect of wettability,' SPE-129012-MS, 2010, doi:10.2118/129012-MS.

Aske, N., *Characterisation of crude oil components, asphaltene aggregation and emulsion stability by means of near infrared spectroscopy and multivariate analysis*, Ph.D. thesis, Norwegian University of Science and Technology, 2002.

Austad, T., Rezaeidoust, A., and Puntervold, T., 'Chemical mechanism of low salinity water flooding in sandstone reservoirs,' SPE-129767-MS, 2010, doi:10.2118/129767-MS.

Bernard, G. G., 'Effect of floodwater salinity on recovery of oil from cores containing clays,' SPE-1725-MS, 1967, doi:10.2118/1725-MS.

Boussour, S., Cissokho, M., Cordier, P., Bertin, H., and Hamon, G., 'Oil recovery by low-salinity brine injection: Laboratory results on outcrop and reservoir cores,' SPE-124277-MS, 2009, doi:10.2118/124277-MS.

Buckley, J. S., Liu, Y., and Monsterleet, S., 'Mechanisms of wetting alteration by crude oils,' SPE-37230-PA, 1997, doi:10.2118/37230-PA.

Cotterill, S. J., *Low Salinity Effects on Oil Recovery*, Master's thesis, Imperial College London, 2014.

Crain, E. R., https://www.spec2000.net/09-relperm.htm, 2015, accessed: 02-04-2018.

Crocker, M. E. and Marchin, L. M., 'Wettability and adsorption characteristics of crude-oil asphaltene and polar fractions,' SPE-14885-PA, 1988, doi:10.2118/14885-PA.

Dake, L. P., *Fundamentals of Reservoir Engineering*, Elsevier Science, 1983, ISBN 9780080568980.

Deer, W. A., Zussman, J., and Howie, R. A., *An introduction to the rock-forming minerals*, Wiley, 1992.

Demirbas, A. and Taylan, O., 'Removing of resins from crude oils,' Petroleum Science and Technology, 2016, doi:10.1080/10916466.2016.1163397.

Emadi, A. and Sohrabi, M., 'Visual investigation of oil recovery by lowsalinity water injection: Formation of water micro-dispersions and wettability alteration,' SPE-166435-MS, 2013, doi:10.2118/166435-MS.

Engelhardt, W. V. and Tunn, W. L. M., *The Flow of Fluids Through Sandstones*, volume 194 of Circular, Illinois State Geological Survey, 1955.

Erke, S. I., Volokitin, Y. E., Edelman, I. Y., Karpan, V. M., Nasralla, R. A., Bondar, M. Y., Mikhaylenko, E. E., and Evseeva, M., 'Low salinity flooding trial at west salym field,' SPE-179629-MS, 2016, doi:10.2118/179629-MS.

Farzaneh, S. A., Carnegie, A., Sohrabi, M., Mills, J. R., Facanha, J. M. F., and Sellers, B., 'A case study of oil recovery improvement by low salinity water injection,' SPE-188512-MS, 2017, doi:10.2118/188512 -MS.

Fjelde, I., Omekeh, A. V., and Sokama-Neuyam, Y. A., 'Low salinity water flooding: Effect of crude oil composition,' SPE-169090-MS, 2014, doi:10.2118/169090-MS.

Fredriksen, S. B., Rognmo, A. U., and FernÃÿ, M. A., 'Pore-scale mechanisms during low salinity waterflooding: Water diffusion and osmosis for oil mobilization,' SPE-180060-MS, 2016, doi:10.2118/180060-MS.

Green, D. W. and Willhite, G. P., *Enhanced Oil Recovery*, Henry L. Doherty Memorial Fund of AIME, Society of Petroleum Engineers, 2008.

Guggenheim, S., 'Definition of clay and clay mineral: Jooint report of the aipea nomenclature and cms nomenclature committees,' Clays and Clay Minerals, 1995, **43**, pp. 255–256.

Hamilton, P. J., *A Review of Radiometric Dating Techniques for Clay Mineral Cements in Sandstones*, Blackwell Publishing Ltd., 2009.

Ishiwata, T., Kurihara, M., Taniguchi, H., Tsuchiya, Y., Watanabe, J., and Matsumoto, K., 'Investigation on low salinity waterflooding through core flooding experiments and numerical simulation,' SPWLA-JFES-2016-M, 2016.

Jadhunandan, P. P. and Morrow, N. R., 'Effect of wettability on waterflood recovery for crude-oil/brine/rock systems,' SPE-22597-PA, 1995, doi:10.2118/22597-PA.

Jerauld, G. R., Webb, K. J., Lin, C.-Y., and Seccombe, J., 'Modeling low-salinity waterflooding,' SPE-102239-MS, 2006, doi:10.2118/102239-MS.

Kakati, A., Jha, N. K., Kumar, G., and Sangwai, J. S., 'Application of low salinity water flooding for light paraffinic crude oil reservoir,' SPE-189249-MS, 2017, doi: 10.2118/189249-MS.

Kantzas, A., Bryan, J., and Taheri, S., http://perminc.com/resources/fundamentals-of-fluid-flow-in-porous-media/chapter-2-the-porous-medium/multi-phase-saturated-rock-properties/wettability/, 2016, accessed: 02-04-2018.

Kumar, H. T., Shehata, A. M., and Nasr-El-Din, H. A., 'Effectiveness of low-salinity and co2 flooding hybrid approaches in low-permeability sandstone reservoirs,' SPE-180875-MS, 2016, doi:10.2118/180875-MS.

Lager, A., Webb, K. J., Black, C. J. J., Singleton, M., and Sorbie, K. S., 'Low salinity oil recovery - an experimental investigation1,' SPWLA-2008-v49n1a2, 2008a, **49**.

Lager, A., Webb, K. J., Collins, I. R., and Richmond, D. M., 'Losal enhanced oil recovery: Evidence of enhanced oil recovery at the reservoir scale,' SPE-113976-MS, 2008b, doi:10.2118/113976-MS.

Ligthelm, D. J., Gronsveld, J., Hofman, J., Brussee, N., Marcelis, F., and Van der Linde, H., 'Novel waterflooding strategy by manipulation of injection brine composition,' SPE-119835-MS, 2009, doi:10.2118/119835-MS.

Mahani, H., Sorop, T. G., Ligthelm, D., Brooks, A. D., Vledder, P., Mozahem, F., and Ali, Y., 'Analysis of field responses to low-salinity waterflooding in secondary and tertiary mode in syria,' SPE-142960-MS, 2011, doi:10.2118/142960-MS.

McGuire, P. L., Chatham, J. R., Paskvan, F. K., Sommer, D. M., and Carini, F. H., 'Low salinity oil recovery: An exciting new eor opportunity for alaska's north slope,' SPE-93903-MS, 2005, doi:10.2118/93903-MS.

Meredith, W., Kelland, S. J., and Jones, D. M., *Influences of biodegradation on crude oil acidity and carboxylic acid composition*, volume 31, Organic Geochemistry, 2000.

Mitchell, D. L. and Speight, J. G., *The solubility of asphaltenes in hydrocarbon solvents*, volume 52, Fuel Sciences Division, 1973.

Miyauchi, T. E. C., Lu, Y., and Firoozabadi, A., 'Low salinity water injection: Effect of acid and base functionality on recovery performance,' SPE-187275-MS, 2017, doi:10.2118/187275-MS.

Morrow, N. R., 'Wettability and its effect on oil recovery,' SPE-21621-PA, 1990, doi: 10.2118/21621-PA.

Nasralla, R. A., Alotaibi, M. B., and Nasr-El-Din, H. A., 'Efficiency of oil recovery by low salinity water flooding in sandstone reservoirs,' SPE-144602-MS, 2011a, doi: 10.2118/144602-MS.

Nasralla, R. A., Bataweel, M. A., and Nasr-El-Din, H. A., 'Investigation of wettability alteration by low salinity water,' SPE-146322-MS, 2011b, doi:10.2118/146322-MS.

Nasralla, R. A. and Nasr-El-Din, H. A., 'Coreflood study of low salinity water injection in sandstone reservoirs,' SPE-149077-MS, 2011, doi:10.2118/149077-MS.

Nasralla, R. A. and Nasr-El-Din, H. A., 'Double-layer expansion: Is it a primary mechanism of improved oil recovery by low-salinity waterflooding?' SPE-154334-MS, 2012, doi:10.2118/154334-MS.

Noureldien, D. M. and Nabil, S., 'Gupco experience with giant fields: Case studies from egypt,' SPE-183556-MS, 2016, doi:10.2118/183556-MS.

Odin, G. S., *Green Marine Clays - Development in Sedimentology*, volume 45, Elsevier, 1988, ISBN 9780080869599.

Pinerez T., I. D., Austad, T., Strand, S., Puntervold, T., Wrobel, S., and Hamon, G., 'Linking low salinity eor effects in sandstone to ph, mineral properties and water composition,' SPE-179625-MS, 2016, doi:10.2118/179625-MS.

Pope, G. A., Lake, L. W., and Helfferich, F. G., 'Cation exchange in chemical flooding: part 1 - basic theory without dispersion,' SPE-142960-MS, 1978, **18**(6), pp. 418–434.

Potter, M. J., 'Vermiculite,' U.S. Geological Survey Minerals Yearbook, 2000, **83**, pp. 1–4.

Pu, H., Xie, X., Yin, P., and Morrow, N. R., 'Low-salinity waterflooding and mineral dissolution,' SPE-134042-MS, 2010, doi:10.2118/134042-MS.

RezaeiDoust, A., Puntervold, T., Strand, S., and Austad, T., 'Smart water as wettability modifier in carbonate and sandstone: A discussion of similarities/differences in the chemical mechanisms,' Energy Fuels, 2009, doi:10.1021/ef900185q.

Robertson, E. P., 'Low-salinity waterflooding to improve oil recovery-historical field evidence,' SPE-109965-MS, 2007, doi:10.2118/109965-MS.

Rotondi, M., Callegaro, C., Masserano, F., and Bartosek, M., 'Low salinity water injection: eniâĂŹs experience,' SPE-171794-MS, 2014, doi:10.2118/171794-MS.

Sandengen, K., Kristoffersen, A., Melhuus, K., and JÃ¿sang, L. O., 'Osmosis as mechanism for low-salinity enhanced oil recovery,' SPE-179741-PA, 2016, doi: 10.2118/179741-PA.

Schulze, D. G., 'Clay minerals,' Clay Minerals, 2005, pp. 246–254.

Seccombe, J., Lager, A., Jerauld, G., Jhaveri, B., Buikema, T., Bassler, S., Denis, J., Webb, K., Cockin, A., and Fueg, E., 'Demonstration of low-salinity eor at interwell scale, endicott field, alaska,' SPE-129692-MS, 2010, doi:10.2118/129692-MS.

Shabib-Asl, A., Ayoub, M. A., and Elraies, K. A., 'Laboratory investigation into wettability alteration by different low salinity water compositions in sandstone rock,' SPE-176492-MS, 2015, doi:10.2118/176492-MS.

Shehata, A. M., Kumar, H. T., and Nasr-El-Din, H. A., 'New insights on relative permeability and initial water saturation effects during low-salinity waterflooding for sandstone reservoirs,' SPE-180874-MS, 2016, doi:10.2118/180874-MS.

Shehata, A. M. and Nasr-El-Din, H. A., 'Spontaneous imbibition study: Effect of connate water composition on low-salinity waterflooding in sandstone reservoirs,' SPE-174063-MS, 2015, doi:10.2118/174063-MS.

Skauge, A., Standal, S., Boe, S., Skauge, T., and Blokhus, A. M., 'Effects of organic acids and bases, and oil composition on wettability,' SPE-56673-MS, 1999, doi: 10.2118/56673-MS.

Sohrabi, M., Mahzari, P., Farzaneh, S. A., Mills, J. R., Tsolis, P., and Ireland, S., 'Novel insights into mechanisms of oil recovery by use of low-salinity-water injection,' SPE-172778-PA, 2017, doi:10.2118/172778-PA.

Sorbo, I. G., *Polar Components in Crude Oils and Their Correlation to Physiochemical Properties*, Master's thesis, University of Bergen, 2016.

Tang, G.-Q. and Morrow, N. R., 'Influence of brine composition and fines migration on crude oil/brine/rock interactions and oil recovery,' Journal of Petroleum Science and Engineering, 1999, **24**, pp. 99–111, ISSN 0920-4105.

Thyne, G. D. and Siyambalagoda Gamage, P. H., 'Evaluation of the effect of low salinity waterflooding for 26 fields in wyoming,' SPE-147410-MS, 2011, doi:10.2118/147410-MS.

Zeinijahromi, A., Ahmetgareev, V., and Bedrikovetsky, P., 'Case study of 25 years of low salinity water injection,' SPE-176128-MS, 2015, doi:10.2118/176128-MS.

Zeinijahromi, A. and Bedrikovetsky, P., 'Fines-migration-assisted oil and gas recovery (low salinity water injection),' SPE-176548-MS, 2015, doi:10.2118/176548-MS.

Zhang, Y., Xie, X., and Morrow, N. R., 'Waterflood performance by injection of brine with different salinity for reservoir cores,' SPE-109849-MS, 2007, doi:10.2118/109849-MS.

VITA

Nadia Ariani earned her undergraduate degree (B. Sc.) in Applied Mathematics from Bandung Institute of Technology, Indonesia in October 2002. After graduation, she was employed by Chevron Indonesia for 11 years, and had different roles as Data Management Specialist, Formation Evaluation Analyst, and Petrophysicist. In May 2018, she received a master degree (M. Sc.) in Petroleum Engineering from Missouri University of Science & Technology, USA.